Journal of Computational Physics **161,** 454–483 (2000)
doi:10.1006/jcph.2000.6504, available online at http://www.idealibrary.com on IDEAL®

Galerkin–Legendre Spectral Method for the 3D Helmholtz Equation

F. Auteri* and L. Quartapelle†

**Dipartimento di Ingegneria Aerospaziale, Politecnico di Milano, Via Lambruschini, 15, 20156 Milano, Italy;*
†*Dipartimento di Fisica, Politecnico di Milano, Piazza Leonardo da Vinci, 32, 20133 Milano, Italy*
E-mail: auteri@aero.polimi.it

Received June 28, 1999; revised March 13, 2000

A Galerkin–Legendre spectral method for the direct solution of Poisson and Helmholtz equations in a three-dimensional rectangular domain is presented. The method extends Jie Shen's algorithm for 2D problems by using the diagonalization of the three mass matrices in the three spatial directions and fully exploits the direct product nature of the spectral approximation. The Dirichlet boundary values are taken into account by means of a discrete lifting performed in three subsequent steps and built upon Gauss–Legendre quadrature points. A few numerical tests illustrate the accuracy and efficiency of the method. © 2000 Academic Press

Key Words: three-dimensional Helmholtz equation; Galerkin–Legendre spectral method; nonhomogeneous Dirichlet condition; lifting of the Dirichlet datum; separation of variables; direct product structure; diagonalization algorithm; direct solution method; fast elliptic spectral solver.

CONTENTS

1. INTRODUCTION

The first implementations of spectral methods using orthogonal polynomials in non-periodic domains were based on Tau–Chebyshev technique [1–3]. For instance, for the

0021-9991/00 $35.00

Poisson and Helmholtz equations of interest here, the early method of solution proposed by Haidvogel and Zang [4] was based on a Tau–Chebyshev approximation. Such a method consists of a direct algorithm for 2D elliptic equations in a rectangular region exploiting the variable separation by means of a diagonalization in one direction; see also [2, p. 133]. This algorithm, together with some iterative versions of it, was subsequently generalized by Haldenwang, *et al.* [5] to solve three-dimensional elliptic problems under general non-homogenous boundary conditions.

In the last ten years, spectral methods have witnessed a growing interest in collocation methods relying upon Lagrangian bases as well as in variational formulations of Galerkin type using Legendre polynomials [6]; see also [7]. In particular, in the context of the Galerkin method, Jie Shen [8] introduced a new basis of Legendre polynomials to solve Helmholtz and biharmonic problems in two dimensions by diagonalization. Shen's basis has the interesting property of being orthogonal in the energy norm (i.e., the L^2 norm of the first derivative of the variable), so that the diagonalization has to be performed on the mass matrix which has a very simple pentadiagonal profile. In Shen's algorithm, the spectral decomposition is performed only in one spatial direction, and the algorithm has been extended also to deal with a spectral representation based on Chebyshev polynomials [9]. As a matter of fact, the mass diagonalization for the Legendre approximation can be applied in both spatial directions. This has been shown by the present authors in [10], where the idea of a fully discrete lifting for enforcing nonhomogeneous Dirichlet boundary conditions for the 2D Helmholtz equation has also been introduced. In fact, in a variational setting the lifting of the Dirichlet data represents, in general, the most appropriate way of accounting for this kind of boundary conditions, cf. Strang and Fix [11], and provides, in particular, the simplest way of accommodating numerically the compatibility conditions existing among the Dirichlet data of the continuum problem, as shown by Bernardi and Maday [6]. For instance, the lifting proposed in [10] for the Galerkin–Legendre spectral approximation of the 2D elliptic equation pivots on the compatibility conditions at the four corners by a two-step process to account for the boundary values prescribed first at the corners and then on the four sides of the rectangular domain.

The aim of this paper is to describe a direct spectral solver for the 3D Helmholtz equation in a rectangular box based on the Galerkin–Legendre spectral approximation. The proposed algorithm relies upon the diagonalization of the three mass matrices in the three spatial directions and uses a lifting of the Dirichlet boundary values which extends the one adopted in two dimensions. Quite obviously, the lifting for the 3D problem will be performed in three steps to account for the corners values, the edge values, and the face values of the Dirichlet condition, the result of each step being required for executing the next one.

As it will be shown in the following, the most complex component of the proposed method is in fact this three-step lifting. The point is that such a lifting is necessary to transform the direct (Cartesian) product structure of the problem in the physical space into the direct product in the space of the Legendre coefficients. In this manner one can build a spectral method for 3D problems relying upon the solution of only one-dimensional subproblems which thus implement the idea of variable separation in the transformed space of Legendre coefficients. The development of the algorithm has required us to introduce a notation suitable for representing all the operations of matrix multiplication which must be performed on the three-dimensional array of the Legendre coefficients of the unknown. The notation proposed in the paper may appear somewhat complex but we have been unable to find an alternative one which could be more convenient for the analysis and the computer

implementation of the new solution method. Such a complexity is not met, of course, when local discretizations, such as those offered by finite differences or elements, are adopted, in which case the standard tensor product notation is sufficient to derive direct solution algorithms for rectangular domains; see, e.g., the classical work by Lynch *et al.* [12].

Anyhow, despite its notational complexity, the proposed three-step lifting for the spectral Galerkin method represents a small fraction of the total computational effort needed to solve a given 3D problem. In fact, as it will be shown by the numerical tests, the solution cost is associated mainly with evaluating the perturbation of the right hand side by the lifting and the similarity transformations that exploit the eigenvector decompositions, letting aside the cost of the initialization phase to obtain the point values of the basis functions for the L^2 projection of the data and to solve the eigenproblems. In this respect, it must be stressed that the perturbation of the right hand side is a step needed in Galerkin as well as in collocation methods based on Gauss–Lobatto grid points. Therefore, the cost of such a perturbation constitutes a bound for any method, either spectral Galerkin or pseudospectral collocation, based on eigenstructure decomposition.

The present paper is organized as follows. In Section 2 we recall the Legendre basis proposed by Shen [8] for approximating differential equations in one dimension, augmented in order to allow a discrete lifting of the prescribed boundary values [10]. Section 3 describes the spectral approximation of the 3D Helmholtz equation supplemented by nonhomogeneous Dirichlet conditions, by means of the Galerkin–Legendre formulation. First, in Subsection 3.1 we define the differential boundary value problem and the spectral expansion of its solution, by introducing a special notation particularly convenient for the representation of the algorithm which fully exploits the variable separation in three dimensions. Then, Subsection 3.2 addresses the issue of compatibility conditions on the Dirichlet boundary values prescribed on the six faces of the 3D rectangular domain. The compatibility conditions allow us to perform the lifting of the nonhomogeneous Dirichlet data in a three-step process described in Subsection 3.3. These steps account for the boundary values specified at the vertices, along the edges and on the faces, in succession, in full compliance with variable separation. The derivation of the basic formulas for the edge and face components of the lifting is relegated in the Appendix, where the set of all of the discrete Dirichlet data used by our lifting is also displayed. The three-step lifting is then used to perturb the right hand side of the system of discrete equations (Subsection 3.4). The homogenized Dirichlet boundary value problem so obtained is finally solved by a triple diagonalization algorithm relying on the eigenstructure of the three 1D mass matrices associated with the Legendre approximation in each spatial direction, as described in Subsection 3.5. A few numerical tests assessing the spectral accuracy of the proposed direct method are presented in Section 4. The last section is devoted to the concluding remarks.

2. GALERKIN–LEGENDRE APPROXIMATION

In this section, the Galerkin–Legendre approximation of a second order linear ODE $-u'' + \gamma u = s(x)$, with γ a nonnegative constant, is considered. The explicit form of the stiffness and mass matrix is given, following the derivation of Shen [8] and including the treatment of nonhomogeneous boundary conditions at the interval extremes.

Let us consider the basis for representing functions of x defined on the interval $[-1, 1]$,

$$\{L_n^*(x), 0 \le n \le N\} \equiv \{1, x/\sqrt{2}, k_{n-1}(1-x^2)L'_{n-1}(x), 2 \le n \le N\},$$

where $k_n \equiv (\sqrt{n+1/2})/(n+n^2)$ and $L_n(x)$, $n = 0, 1, 2, \ldots$, are the Legendre polynomials. Thus $L_n^*(x)$ is a polynomial of degree n for any $n \geq 0$ and, for $n \geq 2$, one has Shen's basis [8]

$$L_n^*(x) = \frac{L_{n-2}(x) - L_n(x)}{\sqrt{2(2n-1)}}, \qquad n \geq 2.$$

The normalization of $L_n^*(x)$ for $n > 0$ has been chosen to make the stiffness matrix coincident with the unit matrix of proper dimension, but for the constant mode. In fact, once the stiffness matrix D is defined by

$$d_{n,k} \equiv \int_{-1}^{1} L_n^*(x)' \, L_k^*(x)' \, dx, \qquad n, k \geq 0,$$

it is immediate to see that

$$\begin{aligned} d_{n,k} &= \delta_{n,k}, \qquad n, k \geq 1, \\ d_{n,0} &= d_{0,n} = 0, \qquad n \geq 0, \end{aligned}$$

$\delta_{n,k}$ being the Kronecker symbol, as a consequence of the Sturm–Liouville equation for Jacobi polynomials and of the normalization

$$\int_{-1}^{1} L_n(x) L_k(x) \, dx = \frac{2}{2n+1} \, \delta_{n,k}, \qquad n, k \geq 0.$$

For further reference, the $(N+1) \times (N+1)$ stiffness matrix is denoted by ${}^0D$ to remind that its leading element $D_{0,0}$ is zero; namely, we write

$$ {}^0D = \begin{array}{c} \\ 0 \\ 1 \\ 2 \\ \vdots \\ N \end{array} \begin{array}{c} \begin{array}{ccccc} 0 & 1 & 2 & \cdots & N \end{array} \\ \begin{pmatrix} 0 & & & & \\ & 1 & & & \\ & & 1 & & \\ & & & \ddots & \\ & & & & 1 \end{pmatrix} \end{array}.$$

Similarly, the $(N+1) \times (N+1)$ mass matrix M is defined by

$$m_{n,k} \equiv \int_{-1}^{1} L_n^*(x) L_k^*(x) \, dx, \qquad n, k \geq 0.$$

By elementary properties of Jacobi polynomials or as demonstrated in [8], the only nonzero elements of M are located along the diagonal and two codiagonals, according to the

pentadiagonal profile,

$$M = \begin{array}{c} \\ 0 \\ 1 \\ 2 \\ 3 \\ 4 \\ \vdots \\ N-2 \\ N-1 \\ N \end{array} \begin{array}{c} \begin{array}{ccccccccc} 0 & 1 & 2 & 3 & 4 & \cdots & N-2 & N-1 & N \end{array} \\ \begin{pmatrix} c_0 & 0 & a_0 & & & & & & \\ 0 & c_1 & 0 & a_1 & & & & & \\ a_0 & 0 & c_2 & 0 & a_2 & & & & \\ & a_1 & 0 & c_3 & 0 & \ddots & & & \\ & & a_2 & 0 & c_4 & 0 & \ddots & & \\ & & & \ddots & 0 & \ddots & 0 & a_{N-3} & \\ & & & & \ddots & 0 & c_{N-2} & 0 & a_{N-2} \\ & & & & & a_{N-3} & 0 & c_{N-1} & 0 \\ & & & & & & a_{N-2} & 0 & c_N \end{pmatrix} \end{array}.$$

A direct calculation gives

$$a_0 = \sqrt{\frac{2}{3}}, \qquad a_1 = \frac{1}{3\sqrt{5}}, \qquad a_n = \frac{-1}{(2n+1)\sqrt{(2n-1)(2n+3)}}, \quad n \geq 2,$$

$$c_0 = 2, \qquad c_1 = \frac{1}{3}, \qquad c_n = \frac{2}{(2n-3)(2n+1)}, \quad n \geq 2.$$

3. THE 3D HELMHOLTZ EQUATION

3.1. *Spectral Approximation of the Helmholtz Equation*

Let us consider the Dirichlet problem for the Helmholtz operator with unknown $u = u(x, y, z)$ in the cubic region $\Omega \equiv (-1, 1)^3$,

$$(-\nabla^2 + \gamma)u = s(x, y, z), \qquad u|_{\partial\Omega} = a(\boldsymbol{r}_{\partial\Omega}),$$

where γ is a nonnegative constant, $s(x, y, z)$ is a known source term defined in Ω, and $a(\boldsymbol{r}_{\partial\Omega})$ is the Dirichlet boundary datum specified on $\partial\Omega$.

The spatial discretization of the Helmholtz equation is done by means of the Galerkin projection method employing the Legendre basis $L_n^*(x), n \geq 0$, defined in Section 2. The approximate solution u_N is expanded in the triple series

$$u_N(x, y, z) = \sum_{i=0}^{I} L_i^*(x) \underbrace{\sum_{k=0}^{K} u_{i,j,k} L_k^*(z)}_{L_j^*(y)} \sum_{j=0}^{J}.$$

Symbol $\sum$ is used to indicate a summation acting on the expression on the left, instead of on the right, as the usual $\sum$. The special symbol $\sum$ was introduced in [10] to be fully adherent with the matrix notation used in [2] for two-dimensional elliptic equations. The present problem being three-dimensional, we introduce also the new symbol $\underbrace{\sum}$ to deal with

the summation along the "third" dimension. Indicating the three summations in the three spatial directions according to this special notation turns out to be particularly convenient in the derivation of the algorithms to be presented below.

3.2. *Compatibility of the Dirichlet Data*

The distribution of the Dirichlet boundary values is specified on the six faces of the rectangular domain Ω. This means that the following six functions, each of two variables, are known for any $|x| \le 1$, $|y| \le 1$, and $|z| \le 1$,

$$\begin{aligned} a^{FX_1}(y,z) &= a(-1,y,z), & a^{FX_2}(y,z) &= a(1,y,z),\\ a^{FY_1}(x,z) &= a(x,-1,z), & a^{FY_2}(x,z) &= a(x,1,z),\\ a^{FZ_1}(x,y) &= a(x,y,-1), & a^{FZ_2}(x,y) &= a(x,y,1). \end{aligned}$$

These functions are *not* independent since they must satisfy compatibility conditions. In fact, as shown by Grisvard [13, Theorem 1.5.1.7], in order for the function $a(\boldsymbol{r}_{\partial\Omega})$ of the Dirichlet datum to be the trace of a function belonging to the Sobolev space $H^1((-1,1)^3)$, it must satisfy a set of compatibility conditions of an integral character. Such conditions reduce themselves to pointwise continuity along the twelve edges of the cube and at the eight vertices, if the datum a can be assumed to be piecewise continuous and bounded, as it is most often in practice.

Let us examine first the set of compatibility conditions along the edges parallel to the x axis and consider in particular the edge $|x| \le 1$, $y = -1$, and $z = -1$. The continuity along this edge means that we have the following constraint between the two functions $a^{FY_1}(x,z) = a(x,-1,z)$ and $a^{FZ_1}(x,y) = a(x,y,-1)$, defined above,

$$a^{FY_1}(x,-1) = a^{FZ_1}(x,-1).$$

This allows us to introduce the one-variable function $a^{ex_1}(x) = a(x,-1,-1)$ representing the distribution of the Dirichlet value along the considered edge, which is the intersection of the two faces. The application of the same argument to all the other edges leads us to define the following twelve functions of only one variable,

$$\begin{aligned} a^{ex_1}(x) &= a(x,-1,-1), & a^{ey_1}(y) &= a(-1,y,-1), & a^{ez_1}(z) &= a(-1,-1,z),\\ a^{ex_2}(x) &= a(x,+1,-1), & a^{ey_2}(y) &= a(+1,y,-1), & a^{ez_2}(z) &= a(+1,-1,z),\\ a^{ex_3}(x) &= a(x,+1,+1), & a^{ey_3}(y) &= a(+1,y,+1), & a^{ez_3}(z) &= a(+1,+1,z),\\ a^{ex_4}(x) &= a(x,-1,+1), & a^{ey_4}(y) &= a(-1,y,+1), & a^{ez_4}(z) &= a(-1,+1,z), \end{aligned}$$

which represent the distribution of the Dirichlet boundary value along the edges of the prism.

The continuity of the Dirichlet data at the eight vertices (called also "corners") of the prism implies that the functions of a single variable just introduced must satisfy compatibility conditions at these eight points. We are therefore led to identify the (unique) value prescribed

at each corner of the prism by defining the corner values

$$\begin{cases} a^{\mathrm{lbn}} = a(-1,-1,-1), & a^{\mathrm{ltn}} = a(-1,1,-1), \\ a^{\mathrm{rbn}} = a(1,-1,-1), & a^{\mathrm{rtn}} = a(1,1,-1), \\ a^{\mathrm{lbf}} = a(-1,-1,1), & a^{\mathrm{ltf}} = a(-1,1,1), \\ a^{\mathrm{rbf}} = a(1,-1,1), & a^{\mathrm{rtf}} = a(1,1,1), \end{cases}$$

where superscripts l and r denote left and right, b and t denote bottom and top, and n and f denote near and far position of the considered corner.

3.3. *Three-Step Lifting of the Dirichlet Data*

In the following we introduce a lifting of the nonhomogeneous Dirichlet condition which accounts in succession for the boundary values specified at the vertices, along the edges and on the faces of the boundary of the rectangular region Ω. As it will become evident later, it is precisely the cascadic account of the Dirichlet boundary data belonging to these three different sets that allows us to develop an algorithm implementing the separation of variables in the space of the Legendre coefficients, and exploiting the direct product nature of the considered spectral approximation.

The lifting of the Dirichlet boundary datum $a(\boldsymbol{r}_{\partial\Omega})$ consists of expressing the solution $u_N(x,y,z)$ in two parts, as

$$u_N(x,y,z) = u_{0,N}(x,y,z) + u_{a,N}(x,y,z),$$

where $u_{0,N}(x,y,z)$ satisfies a homogeneous Dirichlet condition, while $u_{a,N}(x,y,z)$ is an arbitrary function whose trace on $\partial\Omega$ approximates $a(\boldsymbol{r}_{\partial\Omega})$.

To determine the lifting $u_{a,N}(x,y,z)$ we choose to split it in three separate contributions,

$$u_{a,N}(x,y,z) = u_{a,N}^{\mathrm{corners}}(x,y,z) + u_{a,N}^{\mathrm{edges}}(x,y,z) + u_{a,N}^{\mathrm{faces}}(x,y,z),$$

where $u_{a,N}^{\mathrm{corners}}(x,y,z)$ is the component to account for nonzero Dirichlet values at the *corners*, $u_{a,N}^{\mathrm{edges}}(x,y,z)$ is the component to relief nonzero Dirichlet values on the *edges*, and $u_{a,N}^{\mathrm{faces}}(x,y,z)$ is the component to relief nonzero Dirichlet values on the *faces*.

The first component $u_{a,N}^{\mathrm{corners}}(x,y,z)$ is determined by a collocative approach, which enables one to satisfy the Dirichlet boundary condition in a strong sense exclusively at the corners. This is indeed a useful property, especially if the method is used as a starting point for applications to more complex domains via a domain decomposition approach. The second and the third components of the lifting are instead evaluated by the Galerkin–Legendre approach using the L^2 projection of the boundary data. The use of L^2 projections in the proposed way of enforcing the Dirichlet condition can lead to a suboptimal convergence rate of the approximation with respect to the stronger $H^{1/2}$ projection, as pointed out by a reviewer. This lack of optimality is however expected to be barely felt in applications and is anyway compensated by the simplicity of the L^2 projection in the implementation.

The complete lifting including the three components is finally used to perturb the right hand side of the discrete Helmholtz equation to obtain the final system of algebraic equations.

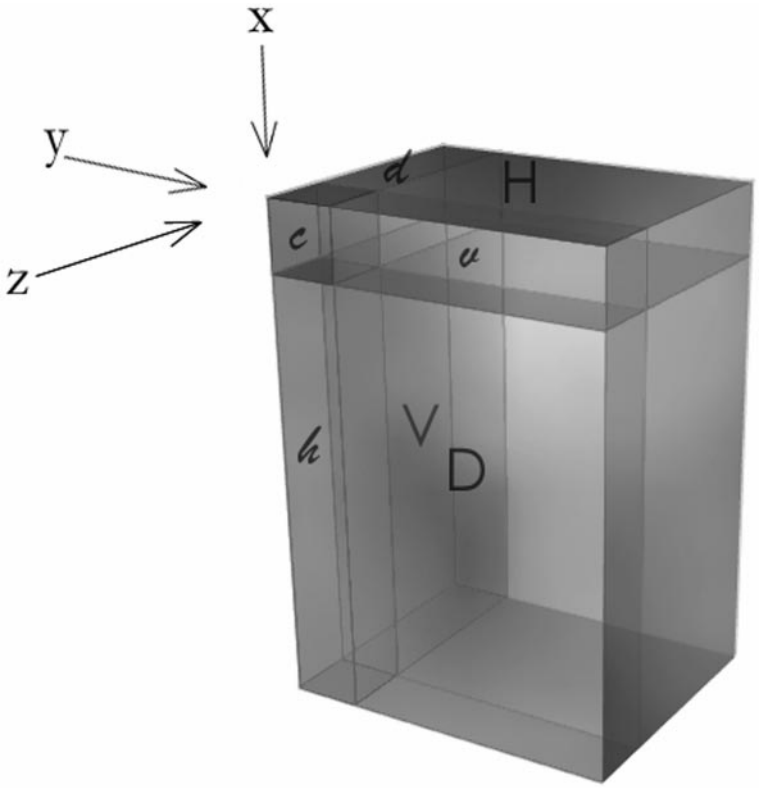

FIG. 1. Partitioning of the array of the expansion coefficients for the 3D Helmholtz problem in a rectangular domain.

It is convenient to introduce the following partitioning of the three-dimensional array[1] of the Legendre coefficients,

$$\boldsymbol{U} = \left(\begin{array}{c|c} \boldsymbol{U}^{(\mathrm{c})} & \boldsymbol{U}^{(\mathrm{v})} \\ \hline \boldsymbol{U}^{(\mathrm{h})} & \boldsymbol{U}^{(\mathrm{D})} \end{array} \quad , \quad \begin{array}{c|c} \boldsymbol{U}^{(\mathrm{d})} & \boldsymbol{U}^{(\mathrm{H})} \\ \hline \boldsymbol{U}^{(\mathrm{V})} & \boldsymbol{U} \end{array} \right) ,$$

where $\boldsymbol{U}^{(\mathrm{c})}$ is the $2 \times 2 \times 2$ array associated with the basis elements which are nonzero on the corners; moreover, $\boldsymbol{U}^{(\mathrm{h})}$, $\boldsymbol{U}^{(\mathrm{v})}$, and $\boldsymbol{U}^{(\mathrm{d})}$ are $(I-1) \times 2 \times 2$, $2 \times (J-1) \times 2$, and $2 \times 2 \times (K-1)$ arrays associated with basis functions which are nonzero respectively on the horizontal, vertical, and in-depth edges of the cube, but for the extremes; then, $\boldsymbol{U}^{(\mathrm{H})}$, $\boldsymbol{U}^{(\mathrm{V})}$, and $\boldsymbol{U}^{(\mathrm{D})}$ are $2 \times (J-1) \times (K-1)$, $(I-1) \times 2 \times (K-1)$, and $(I-1) \times (J-1) \times 2$ arrays associated with basis functions which are nonzero on the square faces of the cubes, normal to the axis x, y, and z, respectively, but vanishing on the sides of each face. Finally, $\boldsymbol{U}$ is the $(I-1) \times (J-1) \times (K-1)$ array which contains the coefficients pertaining only to the "internal modes," that is, modes vanishing on the boundary. The partitioning is shown in Fig. 1. The meaning of the superscripts (h), (v), and (d) is with reference to a system of

[1] In the following, boldface capital letters will always indicate three-dimensional arrays, namely, arrays with three indices, each with a range extent >1. On the contrary, two-dimensional arrays (i.e., ordinary matrices) will be denoted by light (nonbold) capital letters.

Cartesian coordinates with the x axis placed horizontally, the y axis vertically, and the z axis along the depth direction. The naming of the partitioning should not be confused with the actual placement of the rectangular subarrays $\boldsymbol{U}^{(\mathrm{h})}$ and $\boldsymbol{U}^{(\mathrm{v})}$ in the complete array $\boldsymbol{U}$, where the first index corresponds to x and the second index to y according to the standard usage.

By virtue of this partitioning, the array representation of the Legendre coefficients of the lifting $u_{a,N}(x, y, z)$ will be

$$\boldsymbol{U}_a = \left(\begin{array}{c|c} \boldsymbol{U}_a^{(\mathrm{c})} & \boldsymbol{U}_a^{(\mathrm{v})} \\ \hline \boldsymbol{U}_a^{(\mathrm{h})} & \boldsymbol{U}_a^{(\mathrm{D})} \end{array} \right), \quad \left(\begin{array}{c|c} \boldsymbol{U}_a^{(\mathrm{d})} & \boldsymbol{U}_a^{(\mathrm{H})} \\ \hline \boldsymbol{U}_a^{(\mathrm{V})} & \boldsymbol{0} \end{array} \right),$$

where $\boldsymbol{0}$ denotes the zero array of size $(I-1) \times (J-1) \times (K-1)$.

3.3.1. Corner (vertex) component of the lifting. As anticipated, the corner component $u_{a,N}^{\mathrm{corners}}(x, y, z)$ of the lifting (see the left drawing in Fig. 2) is determined by a collocative approach, i.e., we write

$$\begin{cases} u_{a,N}^{\mathrm{corners}}(-1,-1,-1) = a^{\mathrm{lbn}}, & u_{a,N}^{\mathrm{corners}}(-1,1,-1) = a^{\mathrm{ltn}}, \\ u_{a,N}^{\mathrm{corners}}(1,-1,-1) = a^{\mathrm{rbn}}, & u_{a,N}^{\mathrm{corners}}(1,1,-1) = a^{\mathrm{rtn}}, \\ u_{a,N}^{\mathrm{corners}}(-1,-1,1) = a^{\mathrm{lbf}}, & u_{a,N}^{\mathrm{corners}}(-1,1,1) = a^{\mathrm{ltf}}, \\ u_{a,N}^{\mathrm{corners}}(1,-1,1) = a^{\mathrm{rbf}}, & u_{a,N}^{\mathrm{corners}}(1,1,1) = a^{\mathrm{rtf}}. \end{cases}$$

It is natural to seek this part of the lifting in the subspace spanned by the basis functions of (x, y, z) which are nonzero on the corners, namely,

$$\begin{array}{ll} L_0^*(x)L_0^*(y)L_0^*(z) & L_0^*(x)L_1^*(y)L_0^*(z) \\ L_1^*(x)L_0^*(y)L_0^*(z) & L_1^*(x)L_1^*(y)L_0^*(z) \\ L_0^*(x)L_0^*(y)L_1^*(z) & L_0^*(x)L_1^*(y)L_1^*(z) \\ L_1^*(x)L_0^*(y)L_1^*(z) & L_1^*(x)L_1^*(y)L_1^*(z). \end{array}$$

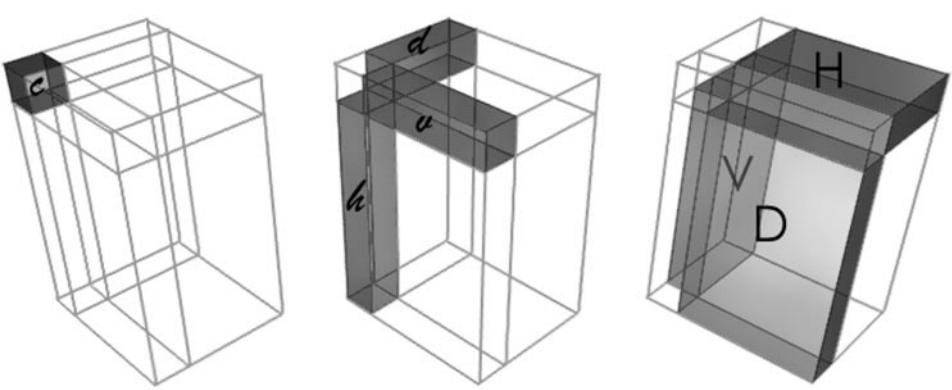

FIG. 2. Schematic representation of the three-step process to lift the Dirichlet condition of a 3D Helmholtz problem in a rectangular domain. Left, corner component; middle, edge component; right, face component.

Accordingly, we have

$$u_{a,N}^{\text{corners}}(x,y,z) = \begin{pmatrix} L_0^*(x) & L_1^*(x) \end{pmatrix} \quad \boldsymbol{U}_a^{(\text{c})} \quad \begin{pmatrix} L_0^*(y) \\ L_1^*(y) \end{pmatrix} \begin{pmatrix} L_0^*(z) \\ L_1^*(z) \end{pmatrix}.$$

We use the notation of placing the matrices associated with the third dimension (z) on the top of the (3D) array to indicate the multiplication "along its third dimension," namely the dimension of the thickness or depth of the array.

Therefore the system of eight equations can be written compactly as

$$\begin{pmatrix} L_0^*(-1) & L_1^*(-1) \\ L_0^*(1) & L_1^*(1) \end{pmatrix} \quad \boldsymbol{U}_a^{(\text{c})} \quad \begin{pmatrix} L_0^*(-1) & L_1^*(-1) \\ L_0^*(1) & L_1^*(1) \end{pmatrix} \begin{pmatrix} L_0^*(-1) & L_0^*(1) \\ L_1^*(-1) & L_1^*(1) \end{pmatrix} = \begin{pmatrix} a^{\text{lbn}} & a^{\text{ltn}} & a^{\text{lbf}} & a^{\text{ltf}} \\ a^{\text{rbn}} & a^{\text{rtn}} & a^{\text{rbf}} & a^{\text{rtf}} \end{pmatrix}$$

and is nonsingular. A simple calculation gives

$$\begin{aligned}
U_a^{(\text{c})}(0,0,0) &= \frac{1}{8}(a^{\text{lbn}} + a^{\text{ltn}} + a^{\text{rbn}} + a^{\text{rtn}} + a^{\text{lbf}} + a^{\text{ltf}} + a^{\text{rbf}} + a^{\text{rtf}}),\\
U_a^{(\text{c})}(1,0,0) &= \frac{1}{4\sqrt{2}}(-a^{\text{lbn}} - a^{\text{ltn}} + a^{\text{rbn}} + a^{\text{rtn}} - a^{\text{lbf}} - a^{\text{ltf}} + a^{\text{rbf}} + a^{\text{rtf}}),\\
U_a^{(\text{c})}(0,1,0) &= \frac{1}{4\sqrt{2}}(-a^{\text{lbn}} + a^{\text{ltn}} - a^{\text{rbn}} + a^{\text{rtn}} - a^{\text{lbf}} + a^{\text{ltf}} - a^{\text{rbf}} + a^{\text{rtf}}),\\
U_a^{(\text{c})}(1,1,0) &= \frac{1}{4}(a^{\text{lbn}} - a^{\text{ltn}} - a^{\text{rbn}} + a^{\text{rtn}} + a^{\text{lbf}} - a^{\text{ltf}} - a^{\text{rbf}} + a^{\text{rtf}}),\\
U_a^{(\text{c})}(0,0,1) &= \frac{1}{4\sqrt{2}}(-a^{\text{lbn}} - a^{\text{ltn}} - a^{\text{rbn}} - a^{\text{rtn}} + a^{\text{lbf}} + a^{\text{ltf}} + a^{\text{rbf}} + a^{\text{rtf}}),\\
U_a^{(\text{c})}(1,0,1) &= \frac{1}{4}(a^{\text{lbn}} + a^{\text{ltn}} - a^{\text{rbn}} - a^{\text{rtn}} - a^{\text{lbf}} - a^{\text{ltf}} + a^{\text{rbf}} + a^{\text{rtf}}),\\
U_a^{(\text{c})}(0,1,1) &= \frac{1}{4}(a^{\text{lbn}} - a^{\text{ltn}} + a^{\text{rbn}} - a^{\text{rtn}} - a^{\text{lbf}} + a^{\text{ltf}} - a^{\text{rbf}} + a^{\text{rtf}}),\\
U_a^{(\text{c})}(1,1,1) &= \frac{1}{2\sqrt{2}}(-a^{\text{lbn}} + a^{\text{ltn}} + a^{\text{rbn}} - a^{\text{rtn}} + a^{\text{lbf}} - a^{\text{ltf}} - a^{\text{rbf}} + a^{\text{rtf}}).
\end{aligned}$$

3.3.2. Edge component of the lifting. Once $\boldsymbol{U}_a^{(\text{c})}$ has been determined, the second step of the lifting consists in evaluating its edge component $u_{a,N}^{\text{edges}}(x,y,z)$, namely, to compute $\boldsymbol{U}_a^{(\text{h})}$, $\boldsymbol{U}_a^{(\text{v})}$, and $\boldsymbol{U}_a^{(\text{d})}$ by means of the (1D) Galerkin–Legendre approach (see the middle drawing in Fig. 2). The function $u_{a,N}^{\text{edges}}(x,y,z)$ will be sought in the subspace spanned by basis functions of $H^1(\Omega)$ that are zero on the corners and nonzero on the edges, and whose trace on the edges is the orthogonal projection, in the sense of the $L^2(-1,1)$ inner-product, of the trace of the boundary datum once the corner nonhomogeneous part has been

subtracted. In other terms, we have to determine $u^{\text{edges}}_{a,N}(x, y, z)$ such that

$$\sum_{\text{edges}} \int_{-1}^{1} v u^{\text{edges}}_{a,N} = \sum_{\text{edges}} \int_{-1}^{1} v\big(a - u^{\text{corners}}_{a,N}\big),$$

where $v(x, y, z)$ represents any function belonging to the same subspace in which $u^{\text{edges}}_{a,N}(x, y, z)$ is sought for.

Writing the boundary integral as the sum of the contributions due to the twelve edges, the orthogonal projection can be written as

$$\sum_{\ell=1}^{4} \left\{ \int_{ex_\ell} v u^{\text{h-edges}}_{a,N} + \int_{ey_\ell} v u^{\text{v-edges}}_{a,N} + \int_{ez_\ell} v u^{\text{d-edges}}_{a,N} \right\}$$
$$= \sum_{\ell=1}^{4} \left\{ \int_{ex_\ell} v\big(a^{ex_\ell} - u^{\text{corners}}_{a,N}\big) + \int_{ey_\ell} v\big(a^{ey_\ell} - u^{\text{corners}}_{a,N}\big) + \int_{ez_\ell} v\big(a^{ez_\ell} - u^{\text{corners}}_{a,N}\big) \right\},$$

where the ex_ℓ, $\ell = 1, \ldots, 4$, denote the set of four edges parallel to the x axis and where we used the notation $u^{\text{h-edges}}_{a,N} = u^{\text{edges}}_{a,N}|_{\cup_{\ell=1}^{4} ex_\ell} = u^{\text{edges}}_{a,N}|_{(x,\pm 1,\pm 1)}$, and similarly in the other two directions.

By virtue of the vanishing of any v at the corners, the contributions due to the horizontal, vertical, and depth direction edges can be uncoupled from each other by choosing test functions which vanish on one set of four parallel edges at a time and by expanding the lifting in the same basis. Eventually, the whole problem separates in three independent subproblems, each of them being associated with four parallel edges,

$$\sum_{\ell=1}^{4} \int_{ex_\ell} v u^{\text{h-edges}}_{a,N} = \sum_{\ell=1}^{4} \int_{ex_\ell} v\big(a^{ex_\ell} - u^{\text{corners}}_{a,N}\big),$$
$$\sum_{\ell=1}^{4} \int_{ey_\ell} v u^{\text{v-edges}}_{a,N} = \sum_{\ell=1}^{4} \int_{ey_\ell} v\big(a^{ey_\ell} - u^{\text{corners}}_{a,N}\big),$$
$$\sum_{\ell=1}^{4} \int_{ez_\ell} v u^{\text{d-edges}}_{a,N} = \sum_{\ell=1}^{4} \int_{ez_\ell} v\big(a^{ez_\ell} - u^{\text{corners}}_{a,N}\big).$$

Let us express each of the three problems in a discrete form and consider first the problem associated with the horizontal edges, which is written more precisely

$$\sum_{\ell=1}^{4} \int_{ex_\ell} v u^{\text{edges}}_{a,N} = \sum_{\ell=1}^{4} \int_{ex_\ell} v\big(a^{ex_\ell} - u^{\text{corners}}_{a,N}\big),$$

with the edge-trace of the functions being understood in the integrals, namely, $v = v|_{ex_\ell}$, $u^{\text{edges}}_{a,N} = u^{\text{edges}}_{a,N}|_{ex_\ell}$ and $u^{\text{corners}}_{a,N} = u^{\text{corners}}_{a,N}|_{ex_\ell}$. A detailed derivation of the solution of the problem associated with the four horizontal edges is given in Appendix A.2. The expression of the final solution can be recast in matrix form by introducing the vector of the Gauss–Legendre weights

$$\mathcal{W} \equiv \{w_g, 1 \le g \le I + 1\},$$

and the array $\mathcal{L}$ of values of the Legendre functions computed at the Gauss–Legendre nodes,[2] namely,

$$\mathcal{L} \equiv \{\mathcal{L}(g,i) = L_i^*(x_g), 1 \le g \le I+1, 0 \le i \le I\}.$$

Moreover, it is necessary to introduce the four vectors of the values of the Dirichlet conditions on the four horizontal edges, $a^{ex_1}(x)$, $a^{ex_2}(x)$, $a^{ex_3}(x)$, and $a^{ex_4}(x)$, evaluated at the same quadrature points,

$$\begin{cases} \mathcal{A}^{ex_1} = \{a^{ex_1}(x_g) = a(x_g,-1,-1),\ 1 \le g \le I+1\} \\ \mathcal{A}^{ex_2} = \{a^{ex_2}(x_g) = a(x_g,+1,-1),\ 1 \le g \le I+1\} \\ \mathcal{A}^{ex_3} = \{a^{ex_3}(x_g) = a(x_g,+1,+1),\ 1 \le g \le I+1\} \\ \mathcal{A}^{ex_4} = \{a^{ex_4}(x_g) = a(x_g,-1,+1),\ 1 \le g \le I+1\}. \end{cases}$$

Finally, we have to introduce the partitioning of the mass matrix,[3]

$$M = \begin{pmatrix} M^{(c)} & M^{(h)T} \\ M^{(h)} & \mathsf{M} \end{pmatrix}.$$

In terms of all these quantities, the subcomponent of the lifting associated with the horizontal edges is achieved by solving the following four uncoupled systems of equations,

$$\mathsf{M}U_a^{(h)}(\cdot,0,0) = \frac{1}{4}\mathcal{L}^T[\mathcal{W} \star (\mathcal{A}^{ex_1} + \mathcal{A}^{ex_2} + \mathcal{A}^{ex_3} + \mathcal{A}^{ex_4})] - M^{(h)}U_a^{(c)}(\cdot,0,0),$$

$$\mathsf{M}U_a^{(h)}(\cdot,1,0) = \frac{1}{2\sqrt{2}}\mathcal{L}^T[\mathcal{W} \star (-\mathcal{A}^{ex_1} + \mathcal{A}^{ex_2} + \mathcal{A}^{ex_3} - \mathcal{A}^{ex_4})] - M^{(h)}U_a^{(c)}(\cdot,1,0),$$

$$\mathsf{M}U_a^{(h)}(\cdot,0,1) = \frac{1}{2\sqrt{2}}\mathcal{L}^T[\mathcal{W} \star (-\mathcal{A}^{ex_1} - \mathcal{A}^{ex_2} + \mathcal{A}^{ex_3} + \mathcal{A}^{ex_4})] - M^{(h)}U_a^{(c)}(\cdot,0,1),$$

$$\mathsf{M}U_a^{(h)}(\cdot,1,1) = \frac{1}{2}\mathcal{L}^T[\mathcal{W} \star (\mathcal{A}^{ex_1} - \mathcal{A}^{ex_2} + \mathcal{A}^{ex_3} - \mathcal{A}^{ex_4})] - M^{(h)}U_a^{(c)}(\cdot,1,1),$$

where the symbol $\star$ denotes the element-by-element multiplication of vectors. It is interesting to remark that, irrespective of the decoupling in four mass matrix problems, for the adopted basis the edge component of the lifting associated with the four horizontal edges cannot be evaluated dealing with the Dirichlet values on each edge independently from the other three edges.

The same procedure can be adopted for the four vertical edges and for the four edges in the depth direction. The result is similar to the former expression by virtue of the direct product nature of the basis provided we introduce a partitioning for the mass matrices N and Q in the y and z direction, as

$$N = \begin{pmatrix} N^{(c)} & N^{(v)} \\ N^{(v)T} & \mathsf{N} \end{pmatrix} \quad \text{and} \quad Q = \begin{pmatrix} Q^{(c)} & Q^{(d)} \\ Q^{(d)T} & \mathsf{Q} \end{pmatrix},$$

[2] Here and in the following, script letters are used to indicate quantities evaluated at, or associated with, Gauss–Legendre quadrature points.

[3] Sans serif letters are used throughout to denote vectors, matrices, and arrays which pertain only to internal modes, that is, to basis functions vanishing at the extremes of the interval.

and define the vector $\nu \equiv \{w_g, 1 \le g \le J+1\}$ containing the weights of the Gauss–Legendre quadrature formula with $J+1$ nodes and the matrix $\mathcal{J} \equiv \{\mathcal{L}(g, j) = L_j^*(x_g), 1 \le g \le J+1, 0 \le j \le J\}$, with similar definitions for $\mathcal{U}$ and $\mathcal{K}$ for the expansion in the z variable. Moreover, we need to introduce the vectors $\mathcal{A}^{ey_\ell}$ and $\mathcal{A}^{ez_\ell}$, $\ell = 1, 2, 3, 4$, according to the definitions given in Appendix A.1. The solution for the four vertical edges reads

$$U_a^{(\mathrm{v})}(0,\cdot,0)\boldsymbol{N} = \frac{1}{4}[(\mathcal{A}^{ey_1} + \mathcal{A}^{ey_2} + \mathcal{A}^{ey_3} + \mathcal{A}^{ey_4}) \star \nu]^T \mathcal{J} - U_a^{(\mathrm{c})}(0,\cdot,0)N^{(\mathrm{v})},$$

$$U_a^{(\mathrm{v})}(1,\cdot,0)\boldsymbol{N} = \frac{1}{2\sqrt{2}}[(-\mathcal{A}^{ey_1} + \mathcal{A}^{ey_2} + \mathcal{A}^{ey_3} - \mathcal{A}^{ey_4}) \star \nu]^T \mathcal{J} - U_a^{(\mathrm{c})}(1,\cdot,0)N^{(\mathrm{v})},$$

$$U_a^{(\mathrm{v})}(0,\cdot,1)\boldsymbol{N} = \frac{1}{2\sqrt{2}}[(-\mathcal{A}^{ey_1} - \mathcal{A}^{ey_2} + \mathcal{A}^{ey_3} + \mathcal{A}^{ey_4}) \star \nu]^T \mathcal{J} - U_a^{(\mathrm{c})}(0,\cdot,1)N^{(\mathrm{v})},$$

$$U_a^{(\mathrm{v})}(1,\cdot,1)\boldsymbol{N} = \frac{1}{2}[(\mathcal{A}^{ey_1} - \mathcal{A}^{ey_2} + \mathcal{A}^{ey_3} - \mathcal{A}^{ey_4}) \star \nu]^T \mathcal{J} - U_a^{(\mathrm{c})}(1,\cdot,1)N^{(\mathrm{v})};$$

while that for the four edges in the depth direction is

$$\overset{Q}{U_a^{(\mathrm{d})}}(0,0,\cdot) = \frac{1}{4}[(\mathcal{A}^{ez_1} + \mathcal{A}^{ez_2} + \mathcal{A}^{ez_3} + \mathcal{A}^{ez_4}) \star \mathcal{U}]^T \mathcal{K} - \overset{Q^{(\mathrm{d})}}{U_a^{(\mathrm{c})}}(0,0,\cdot),$$

$$\overset{Q}{U_a^{(\mathrm{d})}}(1,0,\cdot) = \frac{1}{2\sqrt{2}}[(-\mathcal{A}^{ez_1} + \mathcal{A}^{ez_2} + \mathcal{A}^{ez_3} - \mathcal{A}^{ez_4}) \star \mathcal{U}]^T \mathcal{K} - \overset{Q^{(\mathrm{d})}}{U_a^{(\mathrm{c})}}(1,0,\cdot),$$

$$\overset{Q}{U_a^{(\mathrm{d})}}(0,1,\cdot) = \frac{1}{2\sqrt{2}}[(-\mathcal{A}^{ez_1} - \mathcal{A}^{ez_2} + \mathcal{A}^{ez_3} + \mathcal{A}^{ez_4}) \star \mathcal{U}]^T \mathcal{K} - \overset{Q^{(\mathrm{d})}}{U_a^{(\mathrm{c})}}(0,1,\cdot),$$

$$\overset{Q}{U_a^{(\mathrm{d})}}(1,1,\cdot) = \frac{1}{2}[(\mathcal{A}^{ez_1} - \mathcal{A}^{ez_2} + \mathcal{A}^{ez_3} - \mathcal{A}^{ez_4}) \star \mathcal{U}]^T \mathcal{K} - \overset{Q^{(\mathrm{d})}}{U_a^{(\mathrm{c})}}(1,1,\cdot).$$

In conclusion, the edge component of the lifting requires us to solve $4+4+4$ mass matrix problems of size $(I-1)$, $(J-1)$, and $(K-1)$, respectively. It is important to note that the lifting for the edge boundary values depends on the previously computed result of the corner component. In other words, the corner component of the lifting acts itself as a lifting for performing the edge component of the lifting.

3.3.3. Face component of the lifting. Once $\boldsymbol{U}_a^{(\mathrm{c})}$, $\boldsymbol{U}_a^{(\mathrm{h})}$, $\boldsymbol{U}_a^{(\mathrm{v})}$, and $\boldsymbol{U}_a^{(\mathrm{d})}$ have been determined, the third step of the lifting consists in evaluating its face component $u_{a,N}^{\mathrm{faces}}(x, y, z)$, namely, to compute $\boldsymbol{U}_a^{(\mathrm{H})}$, $\boldsymbol{U}_a^{(\mathrm{V})}$, and $\boldsymbol{U}_a^{(\mathrm{D})}$ by means of the (2D) Galerkin–Legendre approach (see the right drawing in Fig. 2). The function $u_{a,N}^{\mathrm{faces}}(x, y, z)$ will be sought in the subspace spanned by basis functions of $H^1(\Omega)$ that are zero on the corners and on the edges while nonzero on the faces, and whose trace on the faces is the orthogonal projection, in the sense of the $L^2((-1,1)^2)$ inner product, of the trace of the boundary datum once the corner and edge nonhomogeneous parts have been subtracted. In other terms, we have to determine $u_{a,N}^{\mathrm{faces}}(x, y, z)$ such that

$$\int_{\partial\Omega} v u_{a,N}^{\mathrm{faces}} = \int_{\partial\Omega} v\big(a - u_{a,N}^{\mathrm{edges}} - u_{a,N}^{\mathrm{corners}}\big),$$

where $v(x, y, z)$ represents any function belonging to the same subspace in which $u_{a,N}^{\mathrm{faces}}(x, y, z)$ is sought.

Writing the boundary integral as the sum of the contributions due to the six faces, the orthogonal projection can be written as

$$\sum_{\ell=1}^{2}\left\{\int_{FX_\ell} v u_{a,N}^{\text{H-faces}} + \int_{FY_\ell} v u_{a,N}^{\text{V-faces}} + \int_{FZ_\ell} v u_{a,N}^{\text{D-faces}}\right\}$$
$$= \sum_{\ell=1}^{2}\left\{\int_{FX_\ell} v\big(a^{FX_\ell} - u_{a,N}^{\text{edges}} - u_{a,N}^{\text{corners}}\big) \right.$$
$$\left. + \int_{FY_\ell} v\big(a^{FY_\ell} - u_{a,N}^{\text{edges}} - u_{a,N}^{\text{corners}}\big) + \int_{FZ_\ell} v\big(a^{FZ_\ell} - u_{a,N}^{\text{edges}} - u_{a,N}^{\text{corners}}\big)\right\},$$

where FX_ℓ, $\ell = 1, 2$, denote the pair of square faces normal to the x axis and where we introduced the notation $u_{a,N}^{\text{H-faces}} = u_{a,N}^{\text{faces}}|_{FX_1 \cup FX_2} = u_{a,N}^{\text{faces}}|_{(\pm 1, y, z)}$, and similarly for the other two pairs of faces.

By virtue of the vanishing of any v at the corners and on the edges, the contributions due to the horizontal, vertical, and depth direction edges can be uncoupled from each other by choosing test functions which vanish on two sets of parallel faces, among the total of three, at a time and by expanding the lifting in the same basis. Eventually, the whole problem separates into three independent ones, each of them being associated with two parallel faces,

$$\sum_{\ell=1}^{2}\int_{FX_\ell} v u_{a,N}^{\text{H-faces}} = \sum_{\ell=1}^{2}\int_{FX_\ell} v\big(a^{FX_\ell} - u_{a,N}^{\text{edges}} - u_{a,N}^{\text{corners}}\big),$$
$$\sum_{\ell=1}^{2}\int_{FY_\ell} v u_{a,N}^{\text{V-faces}} = \sum_{\ell=1}^{2}\int_{FY_\ell} v\big(a^{FY_\ell} - u_{a,N}^{\text{edges}} - u_{a,N}^{\text{corners}}\big),$$
$$\sum_{\ell=1}^{2}\int_{FZ_\ell} v u_{a,N}^{\text{D-faces}} = \sum_{\ell=1}^{2}\int_{FZ_\ell} v\big(a^{FZ_\ell} - u_{a,N}^{\text{edges}} - u_{a,N}^{\text{corners}}\big).$$

Let us consider the problem associated with the faces whose normal is oriented as the z-axis first, which is written more precisely as

$$\sum_{\ell=1}^{2}\int_{FZ_\ell} v u_{a,N}^{\text{faces}} = \sum_{\ell=1}^{2}\int_{FZ_\ell} v\big(a^{FZ_\ell} - u_{a,N}^{\text{edges}} - u_{a,N}^{\text{corners}}\big),$$

with the trace of functions being understood in the integrals, namely, $v = v|_{FZ_\ell}$, $u_{a,N}^{\text{faces}} = u_{a,N}^{\text{faces}}|_{FZ_\ell}$, $u_{a,N}^{\text{edges}} = u_{a,N}^{\text{edges}}|_{FZ_\ell}$ and $u_{a,N}^{\text{corners}} = u_{a,N}^{\text{corners}}|_{FZ_\ell}$. As shown in Appendix A.3, by introducing the two diagonal matrices of the Gauss–Legendre weights,

$$\mathcal{W} = \begin{pmatrix} w_1 & & & \\ & w_2 & & \\ & & \ddots & \\ & & & w_{I+1} \end{pmatrix} \quad \text{and} \quad \mathcal{V} = \begin{pmatrix} v_1 & & & \\ & v_2 & & \\ & & \ddots & \\ & & & v_{J+1} \end{pmatrix},$$

and the two matrices of the values of the specified functions $a^{FZ_1}(x, y)$ and $a^{FZ_2}(x, y)$ at

the Gauss–Legendre quadrature points on the two considered faces,

$$\begin{cases} \mathcal{A}^{FZ_1} = \{a^{FZ_1}(x_g, y_h) = a(x_g, y_h, -1), 1 \le g \le I+1, 1 \le h \le J+1\}, \\ \mathcal{A}^{FZ_2} = \{a^{FZ_2}(x_g, y_h) = a(x_g, y_h, 1), 1 \le g \le I+1, 1 \le h \le J+1\}, \end{cases}$$

one obtains two uncoupled systems to perform the lifting on the faces orthogonal to the z direction,

$$\begin{aligned} \mathsf{M}U_a^{(\mathrm{D})}(\cdot,\cdot,0)\mathsf{N} &= \frac{1}{2}\mathcal{L}^T\mathcal{W}(\mathcal{A}^{FZ_1}+\mathcal{A}^{FZ_2})\mathcal{V}\mathcal{J} - \mathsf{M}U_a^{(\mathrm{h})}(\cdot,\cdot,0)N^{(\mathrm{v})} \\ &\quad - M^{(\mathrm{h})}U_a^{(\mathrm{v})}(\cdot,\cdot,0)\mathsf{N} - M^{(\mathrm{h})}U_a^{(\mathrm{c})}(\cdot,\cdot,0)N^{(\mathrm{v})}, \\ \mathsf{M}U_a^{(\mathrm{D})}(\cdot,\cdot,1)\mathsf{N} &= \frac{1}{\sqrt{2}}\mathcal{L}^T\mathcal{W}\big(-\mathcal{A}^{FZ_1}+\mathcal{A}^{FZ_2}\big)\mathcal{V}\mathcal{J} - \mathsf{M}U_a^{(\mathrm{h})}(\cdot,\cdot,1)N^{(\mathrm{v})} \\ &\quad - M^{(\mathrm{h})}U_a^{(\mathrm{v})}(\cdot,\cdot,1)\mathsf{N} - M^{(\mathrm{h})}U_a^{(\mathrm{c})}(\cdot,\cdot,1)N^{(\mathrm{v})}. \end{aligned}$$

It must be noticed that the determination of the face component of the lifting is possible only after the other two components, associated with the edges normal to the considered faces and with the corners, have already been determined. In fact the expressions above show that the previously computed $\boldsymbol{U}_a^{(\mathrm{v})}$ and $\boldsymbol{U}_a^{(\mathrm{d})}$ as well as $\boldsymbol{U}_a^{(\mathrm{c})}$ enter the right-hand side of the equations giving the face component of the lifting as a known perturbation: stated in other terms, the arrays of the first two steps of the complete lifting act themselves as a lifting for evaluating the third component of the lifting associated with the faces. It is precisely the very peculiar nested structure of a lifting within the lifting that made the lifting for the three-dimensional equation elusive so far. Finally, one can also remark that, again, irrespective of the decoupling of the two problems for Legendre coefficients associated with the considered two faces, each problem involves the Dirichlet data prescribed on both faces: in other words, the face component of the lifting cannot be evaluated on a face-by-face base.

The same procedure can be adopted for the other two face pairs. The result is similar to the former expression by virtue of the direct product nature of the basis provided we recall the partitioning for the mass matrices N and Q in the y and z direction and introduce the matrices $\mathcal{A}^{FX_\ell}$ and $\mathcal{A}^{FY_\ell}$, $\ell = 1, 2$, of the Dirichlet values at the Gauss–Legendre points belonging to the other two face pairs, as defined in Appendix A.1. The solution for the two faces orthogonal to the y direction reads

$$\begin{aligned} \mathsf{M}\overset{Q}{U}_a^{(\mathrm{V})}(\cdot,0,\cdot) &= \frac{1}{2}\mathcal{L}^T\mathcal{W}\big(\mathcal{A}^{FY_1}+\mathcal{A}^{FY_2}\big)\mathcal{U}\mathcal{K} - \mathsf{M}\overset{Q^{(\mathrm{d})}}{U}_a^{(\mathrm{h})}(\cdot,0,\cdot) \\ &\quad - M^{(\mathrm{h})}\overset{Q}{U}_a^{(\mathrm{d})}(\cdot,0,\cdot) - M^{(\mathrm{h})}\overset{Q^{(\mathrm{d})}}{U}_a^{(\mathrm{c})}(\cdot,0,\cdot), \\ \mathsf{M}\overset{Q}{U}_a^{(\mathrm{V})}(\cdot,1,\cdot) &= \frac{1}{\sqrt{2}}\mathcal{L}^T\mathcal{W}\big(-\mathcal{A}^{FY_1}+\mathcal{A}^{FY_2}\big)\mathcal{U}\mathcal{K} - \mathsf{M}\overset{Q^{(\mathrm{d})}}{U}_a^{(\mathrm{h})}(\cdot,1,\cdot) \\ &\quad - M^{(\mathrm{h})}\overset{Q}{U}_a^{(\mathrm{d})}(\cdot,1,\cdot) - M^{(\mathrm{h})}\overset{Q^{(\mathrm{d})}}{U}_a^{(\mathrm{c})}(\cdot,1,\cdot), \end{aligned}$$

while that for the two faces orthogonal to the x direction is

$$\overset{Q}{U}{}_a^{(\mathrm{H})}(0,\cdot,\cdot)\,\boldsymbol{N} = \frac{1}{2}\mathcal{J}^T\mathcal{V}\big(\mathcal{A}^{FX_1}+\mathcal{A}^{FX_2}\big)\mathcal{U}\mathcal{K} - \overset{Q^{(\mathrm{d})}}{U}{}_a^{(\mathrm{v})}(0,\cdot,\cdot)\,\boldsymbol{N} - \overset{Q}{U}{}_a^{(\mathrm{d})}(0,\cdot,\cdot)\,N^{(\mathrm{v})} - \overset{Q^{(\mathrm{d})}}{U}{}_a^{(\mathrm{c})}(0,\cdot,\cdot)\,N^{(\mathrm{v})},$$

$$\overset{Q}{U}{}_a^{(\mathrm{H})}(1,\cdot,\cdot)\,\boldsymbol{N} = \frac{1}{\sqrt{2}}\mathcal{J}^T\mathcal{V}\big(-\mathcal{A}^{FX_1}+\mathcal{A}^{FX_2}\big)\mathcal{U}\mathcal{K} - \overset{Q^{(\mathrm{d})}}{U}{}_a^{(\mathrm{v})}(1,\cdot,\cdot)\,\boldsymbol{N} - \overset{Q}{U}{}_a^{(\mathrm{d})}(1,\cdot,\cdot)\,N^{(\mathrm{v})} - \overset{Q^{(\mathrm{d})}}{U}{}_a^{(\mathrm{c})}(1,\cdot,\cdot)\,N^{(\mathrm{v})}.$$

In conclusion, the face component of the lifting requires us to solve $2+2+2$ two-dimensional mass matrix problems; each of these problems is solved, considering for instance the faces normal to the z axis, by solving $(I-1)$ and $(J-1)$ uncoupled one-dimensional mass matrix problems of size $(J-1)$ and $(I-1)$, respectively.

3.4. *Perturbation of the Right-Hand Side*

The lifting of the Dirichlet datum can be seen as a perturbation on the right-hand side of the linear system of the discretized version of the Helmholtz equation.

Consider first the Helmholtz equation written in weak form after integration by parts,

$$(\boldsymbol{\nabla}(L_i^*L_j^*L_k^*),\boldsymbol{\nabla}u_N)+\gamma(L_i^*L_j^*L_k^*,u_N) = (L_i^*L_j^*L_k^*,s)+\oint_{\partial\Omega} L_i^*L_j^*L_k^*\frac{\partial u_N}{\partial n},$$

for $0\le(i,j,k)\le(I,J,K)$, where the shorthand $L_i^*L_j^*L_k^* = L_i^*(x)L_j^*(y)L_k^*(z)$ has been used and the basis functions have been already put in place of the generic test function. Recalling the lifting $u_N = u_{0,N}+u_{a,N}$, the weak Helmholtz equation above in matrix form reads

$$\overset{Q}{D}\,\boldsymbol{U}N + M\overset{Q}{\boldsymbol{U}}\overset{0}{E} + M\overset{0}{\boldsymbol{F}}\boldsymbol{U}N + \gamma\, M\overset{Q}{\boldsymbol{U}}N = \boldsymbol{S} + \text{boundary integral},$$

where $\boldsymbol{U}=\boldsymbol{U}_0+\boldsymbol{U}_a$, $\overset{0}{E}$ and $\overset{0}{F}$ are the y- and z-counterpart of matrix $\overset{0}{D}$, and $\boldsymbol{S}$ represents the L^2 projection of the source $s(x,y,z)$ onto the Legendre basis, namely, $s_{i,j,k} = (L_i^*(x)L_j^*(y)L_k^*(z), s(x,y,z))$, $0\le(i,j,k)\le(I,J,K)$, the integral being evaluated numerically by means of the direct-product Gauss–Legendre quadrature formula.

We have to note that a convention is implicit in the hybrid array/matrix expressions, as the one written above. It is always understood that any matrix (always denoted by a nonbold capital letter) that acts on a (three-dimensional) array (always denoted by bold capital letter) actually multiplies all the planes with the other array index, not involved in the matrix multiplication, fixed. This is illustrated in Fig. 3.

Since the Dirichlet condition is taken into account by the lifting, only the test functions vanishing on the boundary are needed, represented by the *internal* basis functions $L_i^*(x)L_j^*(y)L_k^*(z)$ for $2\le(i,j,k)\le(I,J,K)$. By exploiting the array and matrix

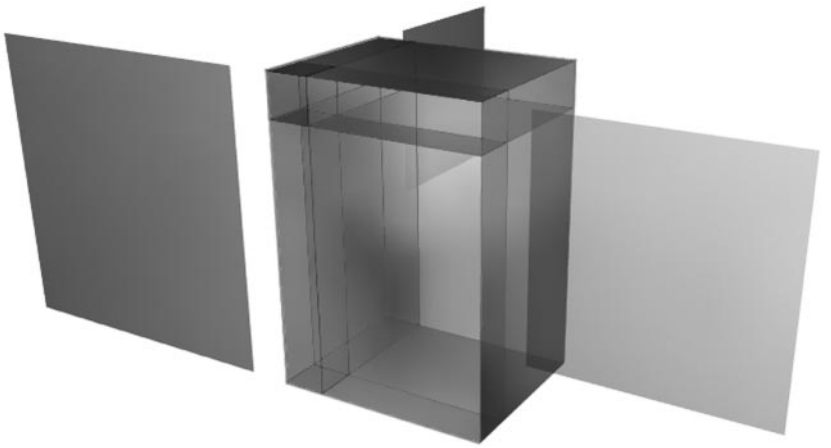

FIG. 3. Schematic of the matrix multiplication structure of the 3D Helmholtz problem discretized by the Galerkin–Legendre spectral method.

partitionings introduced before, the system of equations pertaining to these functions assumes the form

$$\begin{pmatrix} D^{(\mathrm{h})} & \boldsymbol{D} \end{pmatrix} \quad \boldsymbol{U} \quad \begin{pmatrix} Q^{(\mathrm{d})} \\ \boldsymbol{Q} \end{pmatrix} \begin{pmatrix} N^{(\mathrm{v})} \\ \boldsymbol{N} \end{pmatrix} + \begin{pmatrix} M^{(\mathrm{h})} & \boldsymbol{M} \end{pmatrix} \quad \boldsymbol{U} \quad \begin{pmatrix} Q^{(\mathrm{d})} \\ \boldsymbol{Q} \end{pmatrix} \begin{pmatrix} E^{(\mathrm{v})} \\ \boldsymbol{E} \end{pmatrix}$$

$$+ \begin{pmatrix} M^{(\mathrm{h})} & \boldsymbol{M} \end{pmatrix} \quad \boldsymbol{U} \quad \begin{pmatrix} F^{(\mathrm{d})} \\ \boldsymbol{F} \end{pmatrix} \begin{pmatrix} N^{(\mathrm{v})} \\ \boldsymbol{N} \end{pmatrix} + \gamma \begin{pmatrix} M^{(\mathrm{h})} & \boldsymbol{M} \end{pmatrix} \quad \boldsymbol{U} \quad \begin{pmatrix} Q^{(\mathrm{d})} \\ \boldsymbol{Q} \end{pmatrix} \begin{pmatrix} N^{(\mathrm{v})} \\ \boldsymbol{N} \end{pmatrix} = \boldsymbol{S},$$

where

$$\boldsymbol{U} = \boldsymbol{U}_a + \boldsymbol{U}_0 = \left(\begin{array}{c|c} \boldsymbol{U}_a^{(\mathrm{c})} & \boldsymbol{U}_a^{(\mathrm{v})} \\ \hline \boldsymbol{U}_a^{(\mathrm{h})} & \boldsymbol{U}_a^{(\mathrm{D})} \end{array} \right. , \left. \begin{array}{c|c} \boldsymbol{U}_a^{(\mathrm{d})} & \boldsymbol{U}_a^{(\mathrm{H})} \\ \hline \boldsymbol{U}_a^{(\mathrm{V})} & \boldsymbol{U} \end{array} \right).$$

The right-hand side $\boldsymbol{S}$ is the L^2 projection of the source term onto the basis functions pertaining only to the internal Legendre modes. Similarly, all other sans serif letters appearing in the last two equations are defined by

$$\begin{aligned} \boldsymbol{U} &= \{u_{i,j,k}, 2 \le (i, j, k) \le (I, J, K)\}, \\ \boldsymbol{M} &= \{m_{i,i'} = (L_i^*(x), L_{i'}^*(x)), 2 \le (i, i') \le I\}, \\ \boldsymbol{N} &= \{n_{j,j'} = (L_j^*(y), L_{j'}^*(y)), 2 \le (j, j') \le J\}, \\ \boldsymbol{Q} &= \{q_{k,k'} = (L_k^*(z), L_{k'}^*(z)), 2 \le (k, k') \le K\}, \end{aligned}$$

and therefore involves only the internal Legendre modes in each spatial direction.

Since all the elements of $\boldsymbol{U}_a^{(c)}$, $\boldsymbol{U}_a^{(h)}$, $\boldsymbol{U}_a^{(v)}$, $\boldsymbol{U}_a^{(d)}$, $\boldsymbol{U}_a^{(H)}$, $\boldsymbol{U}_a^{(V)}$, and $\boldsymbol{U}_a^{(D)}$ are known, the equation above can be rewritten transferring all the terms involving known quantities in the right-hand side. In particular, for the Legendre basis we are working with, the submatrices $D^{(h)}$, $E^{(v)}$, and $F^{(d)}$ are null and the matrices $\boldsymbol{D}$, $\boldsymbol{E}$, and $\boldsymbol{F}$ of the internal diagonal component are identity matrices of suitable dimension. This implies a substantial simplification of the explicit expression of the four terms contained in the three-dimensional Helmholtz equation. Considering the first term, we find

$$\begin{pmatrix} D^{(h)} & \boldsymbol{D} \end{pmatrix} \quad \begin{matrix} \begin{pmatrix} Q^{(d)} \\ \boldsymbol{Q} \end{pmatrix} \\ \boldsymbol{U} \end{matrix} \quad \begin{pmatrix} N^{(v)} \\ \boldsymbol{N} \end{pmatrix} = \overset{Q^{(d)}}{\boldsymbol{U}_a^{(h)}} N^{(v)} + \overset{Q^{(d)}}{\boldsymbol{U}_a^{(D)}} \boldsymbol{N} + \overset{\boldsymbol{Q}}{\boldsymbol{U}_a^{(V)}} N^{(v)} + \overset{\boldsymbol{Q}}{\boldsymbol{U}} \boldsymbol{N},$$

since matrix $D^{(h)}$ is null and $\boldsymbol{D}$ is simply the identity matrix of dimension $I-1$. A similar calculation for the two derivative terms in the other directions y and z gives

$$\begin{pmatrix} M^{(h)} & \boldsymbol{M} \end{pmatrix} \quad \begin{matrix} \begin{pmatrix} Q^{(d)} \\ \boldsymbol{Q} \end{pmatrix} \\ \boldsymbol{U} \end{matrix} \quad \begin{pmatrix} E^{(v)} \\ \boldsymbol{E} \end{pmatrix} = M^{(h)} \overset{Q^{(d)}}{\boldsymbol{U}_a^{(v)}} + \boldsymbol{M} \overset{Q^{(d)}}{\boldsymbol{U}_a^{(D)}} + M^{(h)} \overset{\boldsymbol{Q}}{\boldsymbol{U}_a^{(H)}} + \boldsymbol{M} \overset{\boldsymbol{Q}}{\boldsymbol{U}}$$

and

$$\begin{pmatrix} M^{(h)} & \boldsymbol{M} \end{pmatrix} \quad \begin{matrix} \begin{pmatrix} F^{(d)} \\ \boldsymbol{F} \end{pmatrix} \\ \boldsymbol{U} \end{matrix} \quad \begin{pmatrix} N^{(v)} \\ \boldsymbol{N} \end{pmatrix} = M^{(h)} \boldsymbol{U}_a^{(d)} N^{(v)} + \boldsymbol{M} \boldsymbol{U}_a^{(v)} N^{(v)} + M^{(h)} \boldsymbol{U}_a^{(H)} \boldsymbol{N} + \boldsymbol{M} \boldsymbol{U} \boldsymbol{N}.$$

The calculation of the nonderivative term proportional to γ is slightly more complicated and gives

$$\begin{pmatrix} M^{(h)} & \boldsymbol{M} \end{pmatrix} \quad \begin{matrix} \begin{pmatrix} Q^{(d)} \\ \boldsymbol{Q} \end{pmatrix} \\ \boldsymbol{U} \end{matrix} \quad \begin{pmatrix} N^{(v)} \\ \boldsymbol{N} \end{pmatrix} = \begin{aligned} &\overset{Q^{(d)}}{M^{(h)} \boldsymbol{U}_a^{(c)}} N^{(v)} + \overset{Q^{(d)}}{\boldsymbol{M}\, \boldsymbol{U}_a^{(h)}} N^{(v)} + \overset{Q^{(d)}}{M^{(h)} \boldsymbol{U}_a^{(v)}} \boldsymbol{N} + \overset{Q^{(d)}}{\boldsymbol{M}\, \boldsymbol{U}_a^{(D)}} \boldsymbol{N} \\ &+ \overset{\boldsymbol{Q}}{M^{(h)} \boldsymbol{U}_a^{(d)}} N^{(v)} + \overset{\boldsymbol{Q}}{\boldsymbol{M}\, \boldsymbol{U}_a^{(V)}} N^{(v)} + \overset{\boldsymbol{Q}}{M^{(h)} \boldsymbol{U}_a^{(H)}} \boldsymbol{N} + \overset{\boldsymbol{Q}}{\boldsymbol{M}\, \boldsymbol{U}} \boldsymbol{N}. \end{aligned}$$

The final system of discrete equations to be solved assumes the form

$$\overset{Q}{\boldsymbol{U}} \boldsymbol{N} + \boldsymbol{M} \overset{Q}{\boldsymbol{U}} + \boldsymbol{M} \overset{Q}{\boldsymbol{U}} \boldsymbol{N} + \gamma \boldsymbol{M} \overset{Q}{\boldsymbol{U}} \boldsymbol{N} = \boldsymbol{R},$$

where the perturbed right-hand side includes the lifting according to the definition

$$\begin{aligned}\boldsymbol{R} = \boldsymbol{S} &- \overset{Q^{(\mathrm{d})}}{\boldsymbol{U}_a^{(\mathrm{h})}} N^{(\mathrm{v})} - \overset{Q^{(\mathrm{d})}}{\boldsymbol{U}_a^{(\mathrm{D})}} \boldsymbol{N} - \overset{Q}{\boldsymbol{U}_a^{(\mathrm{V})}} N^{(\mathrm{v})} - M^{(\mathrm{h})} \overset{Q^{(\mathrm{d})}}{\boldsymbol{U}_a^{(\mathrm{v})}} - \boldsymbol{M} \overset{Q^{(\mathrm{d})}}{\boldsymbol{U}_a^{(\mathrm{D})}} \\ &- M^{(\mathrm{h})} \overset{Q}{\boldsymbol{U}_a^{(\mathrm{H})}} - M^{(\mathrm{h})} \boldsymbol{U}_a^{(\mathrm{d})} N^{(\mathrm{v})} - \boldsymbol{M} \boldsymbol{U}_a^{(\mathrm{V})} N^{(\mathrm{v})} - M^{(\mathrm{h})} \boldsymbol{U}_a^{(\mathrm{H})} \boldsymbol{N} \\ &- \gamma \left\{ M^{(\mathrm{h})} \overset{Q^{(\mathrm{d})}}{\boldsymbol{U}_a^{(\mathrm{c})}} N^{(\mathrm{v})} + \boldsymbol{M} \overset{Q^{(\mathrm{d})}}{\boldsymbol{U}_a^{(\mathrm{h})}} N^{(\mathrm{v})} + M^{(\mathrm{h})} \overset{Q^{(\mathrm{d})}}{\boldsymbol{U}_a^{(\mathrm{v})}} \boldsymbol{N} + M^{(\mathrm{h})} \overset{Q}{\boldsymbol{U}_a^{(\mathrm{d})}} N^{(\mathrm{v})} \right. \\ &\qquad \left. + \boldsymbol{M} \overset{Q^{(\mathrm{d})}}{\boldsymbol{U}_a^{(\mathrm{D})}} \boldsymbol{N} + \boldsymbol{M} \overset{Q}{\boldsymbol{U}_a^{(\mathrm{V})}} N^{(\mathrm{v})} + M^{(\mathrm{h})} \overset{Q}{\boldsymbol{U}_a^{(\mathrm{H})}} \boldsymbol{N} \right\}.\end{aligned}$$

From the computational viewpoint, the perturbation of the right-hand side given by the expression above is not too expensive to be evaluated, since, for the considered Galerkin–Legendre method, the matrices corresponding to all the off-diagonal blocks contain only two nonzero elements and the three matrices $\boldsymbol{M}$, $\boldsymbol{N}$, and $\boldsymbol{Q}$ are pentadiagonal, with only three nonzero diagonals. The matrix expression is however a result of a general validity, irrespective of the basis adopted.

3.5. *Mass-Matrix-Based Triple Diagonalization Algorithm*

To solve this linear system, in a preliminary step we solve the symmetric eigenvalue problem [14] for the three pentadiagonal mass matrices $\boldsymbol{M}$, $\boldsymbol{N}$, and $\boldsymbol{Q}$, namely,

$$\begin{aligned} \boldsymbol{M}\boldsymbol{w}^{(i)} &= \lambda_i \boldsymbol{w}^{(i)}, \qquad 2 \le i \le I, \boldsymbol{W} \equiv \left[\boldsymbol{w}^{(2)}, \ldots, \boldsymbol{w}^{(I)}\right], \\ \boldsymbol{N}\boldsymbol{v}^{(j)} &= \sigma_j \boldsymbol{v}^{(j)}, \qquad 2 \le j \le J, \boldsymbol{V} \equiv \left[\boldsymbol{v}^{(2)}, \ldots, \boldsymbol{v}^{(J)}\right], \\ \boldsymbol{Q}\boldsymbol{z}^{(k)} &= \theta_k \boldsymbol{z}^{(k)}, \qquad 2 \le k \le K, \boldsymbol{Z} \equiv \left[\boldsymbol{z}^{(2)}, \ldots, \boldsymbol{z}^{(K)}\right], \end{aligned}$$

so that

$$\boldsymbol{W}^T \boldsymbol{M} \boldsymbol{W} = \Lambda, \qquad \boldsymbol{V}^T \boldsymbol{N} \boldsymbol{V} = \Sigma, \qquad \boldsymbol{Z}^T \boldsymbol{Q} \boldsymbol{Z} = \Theta,$$

where Λ, Σ, and Θ denote the diagonal matrices of the eigenvalues of $\boldsymbol{M}$, $\boldsymbol{N}$, and $\boldsymbol{Q}$, respectively.

As a consequence of the triple similarity transformation

$$\boldsymbol{R} \to \underline{\boldsymbol{R}} = \boldsymbol{W}^T \overset{Z}{\boldsymbol{R}} \boldsymbol{V}$$

and of the analogous one for $\boldsymbol{U}$, the linear system becomes

$$\overset{\Theta}{\underline{\boldsymbol{U}}}\Sigma + \Lambda \overset{\Theta}{\underline{\boldsymbol{U}}} + \Lambda \underline{\boldsymbol{U}} \Sigma + \gamma \Lambda \overset{\Theta}{\underline{\boldsymbol{U}}} \Sigma = \underline{\boldsymbol{R}},$$

which is solved, componentwise, by means of

$$\underline{\boldsymbol{U}}_{i,j,k} = \frac{\underline{\boldsymbol{r}}_{i,j,k}}{\sigma_j\theta_k + \lambda_i\theta_k + \lambda_i\sigma_j + \gamma\lambda_i\sigma_j\theta_k}, \qquad 2 \le (i, j, k) \le (I, J, K).$$

The sought for solution is then obtained by computing the anti-transform

$$\underline{\boldsymbol{U}} \to \boldsymbol{U} = W \overset{Z^T}{\underline{\boldsymbol{U}}} V^T$$

and finally merging $\boldsymbol{U}$ with the precomputed Legendre coefficients of the lifting $u_{a,N}(x, y, z)$, to give

$$\boldsymbol{U} = \left(\begin{array}{c|c} \boldsymbol{U}_a^{(c)} & \boldsymbol{U}_a^{(v)} \\ \hline \boldsymbol{U}_a^{(h)} & \boldsymbol{U}_a^{(D)} \end{array}, \begin{array}{c|c} \boldsymbol{U}_a^{(d)} & \boldsymbol{U}_a^{(H)} \\ \hline \boldsymbol{U}_a^{(V)} & \boldsymbol{U} \end{array}\right).$$

4. NUMERICAL TESTS

The proposed direct solution algorithm for the 3D Helmholtz equation has been implemented exploiting the matrix/array notation described in the previous sections. Despite the complexity of the expression defining the lifted right-hand side $\boldsymbol{R}$ its implementation is relatively straightforward once suitable primitives are introduced to perform the *sparse* matrix multiplications in the three directions, taking into account the block partitioning of the mass matrices.

The first test case we solved is the Dirichlet problem for the Helmholtz equation with exact solution

$$u(x, y, z) = \cos(\pi x)\cos(\pi y)\cos(\pi z)$$

in the domain $\Omega = (-1, 1)^3$, for $\gamma = 100$. The results for the maximum pointwise value of the error $u_N - u$ are presented in Table I and illustrate the spectral accuracy of the method.

The algorithm can applied to any rectangular domain by introducing suitable scaling coefficients associated to the three directions in the expression for $\boldsymbol{R}$ as well as in the triple diagonalization explicit solution formula. This is shown by solving the same problem in the shifted and rescaled box $\Omega = (-\frac{3}{2}, \frac{3}{4}) \times (-\frac{1}{4}, \frac{5}{4}) \times (0.3, 2.2)$. Error results given in Table II confirm the spectral convergence.

TABLE I

Maximum Pointwise Error for the Solution $u = \cos(\pi x)\cos(\pi y)\cos(\pi z)$, $\Omega = (-1, 1)^3$, $\gamma = 100$

$I \times J \times K$	$\|u_N - u\|_\infty$
$6 \times 6 \times 6$	8.11×10^{-3}
$12 \times 12 \times 12$	8.11×10^{-8}
$18 \times 18 \times 18$	5.99×10^{-14}
$24 \times 24 \times 24$	8.36×10^{-14}
$12 \times 15 \times 18$	2.85×10^{-8}

TABLE II
Maximum Pointwise Error for the Solution $u = \cos(\pi x)\cos(\pi y)\cos(\pi z)$, $\Omega = (-\frac{3}{2}, \frac{3}{4}) \times (-\frac{1}{4}, \frac{5}{4}) \times (0.3, 2.2)$, $\gamma = 100$

$I \times J \times K$	$\|u_N - u\|_\infty$
$6 \times 6 \times 6$	1.59×10^{-2}
$12 \times 12 \times 12$	5.54×10^{-7}
$18 \times 18 \times 18$	8.07×10^{-13}
$24 \times 24 \times 24$	3.20×10^{-14}
$12 \times 15 \times 18$	4.92×10^{-7}

Finally, a more challenging problem has been addressed in order to check the capability of the numerical scheme for very high degree bases. We consider a Dirichlet–Helmholtz problem with exact solution

$$u(x, y, z) = \tanh(\alpha \boldsymbol{k} \cdot (\boldsymbol{r} - \boldsymbol{r}_0)),$$

where $\boldsymbol{r} = x\hat{\boldsymbol{x}} + y\hat{\boldsymbol{y}} + z\hat{\boldsymbol{z}}$, while α, $\boldsymbol{k}$, and $\boldsymbol{r}_0$ are constant quantities. This solution corresponds to a plane transition layer of thickness $1/\alpha$ normal to the direction of $\boldsymbol{k}$ and passing through the point $\boldsymbol{r}_0$. Considering the domain $\Omega = (-1, 1)^3$ and taking $\boldsymbol{r}_0 = (1, 1, 1)$, we corner this layer in the region of the "trf" vertex. The results for $\alpha = 50$ and $\boldsymbol{k} = (1, 2, 3)$ are given in Table III in terms of L^∞ and L^2 norms of $u_N - u$. The spectral convergence obtained in this test demonstrates the correctness of the boundary condition treatment in the corner regions by the proposed lifting. The high accuracy is obtained thanks to the increasing resolution of the Legendre basis near the boundary.

In fact, despite the spectral convergence, the accuracy is lower when the transition layer is located in the interior of the domain, as shown by the results reported in Table IV for the test case with $\boldsymbol{k} = (1, 1, 1)$ and $\boldsymbol{r}_0 = (\frac{3}{4}, \frac{3}{4}, \frac{3}{4})$.

The efficiency characteristics of the method are outlined by reporting the dependence of the execution times on the number of unknowns, in Fig. 4. Here the total CPU time versus $N = I = J = K$ is compared with the N^3 and N^4 slopes, the latter being the expected asymptotic behaviour on account of the computational complexity of the similarity transformation component of the algorithm. The performance is better than expected and this may be a consequence of the super-scalar capability of the processor of the workstation (HP-J2240) employed for the tests.

The relative computer cost of the different components of the algorithm are shown in Table V. It is interesting to note that the time needed to perform the lifting is only a small

TABLE III
Errors for $u = \tanh(\alpha \boldsymbol{k} \cdot (\boldsymbol{r} - \boldsymbol{r}_0))$, with $\alpha = 50$, $\boldsymbol{k} = (1, 2, 3)$, and $\boldsymbol{r}_0 = (1, 1, 1)$

$I = J = K$	$\|u_N - u\|_\infty$	$\|u_N - u\|_2$
50	1.49×10^{-2}	4.16×10^{-6}
100	5.69×10^{-5}	1.06×10^{-8}
150	6.07×10^{-7}	5.61×10^{-11}

TABLE IV
Errors for $u = \tanh(\alpha \boldsymbol{k} \cdot (\boldsymbol{r} - \boldsymbol{r}_0))$, with $\alpha = 50$, $\boldsymbol{k} = (1, 1, 1)$, and $\boldsymbol{r}_0 = (\frac{3}{4}, \frac{3}{4}, \frac{3}{4})$

$I = J = K$	$\|u_N - u\|_\infty$	$\|u_N - u\|_2$
50	1.83	6.83×10^{-2}
100	6.27×10^{-2}	1.85×10^{-3}
150	6.92×10^{-3}	1.70×10^{-4}
200	1.71×10^{-3}	2.58×10^{-5}

TABLE V
Partial and Total CPU Times in Seconds

$I = J = K$	Start	Lifting	Perturb.	Solution	Total
25	0.12	0.04	0.14	0.04	0.34
50	1.00	0.23	1.51	0.69	3.43
100	11.02	1.30	13.99	11.33	37.64
150	37.92	3.69	51.76	41.94	135.31

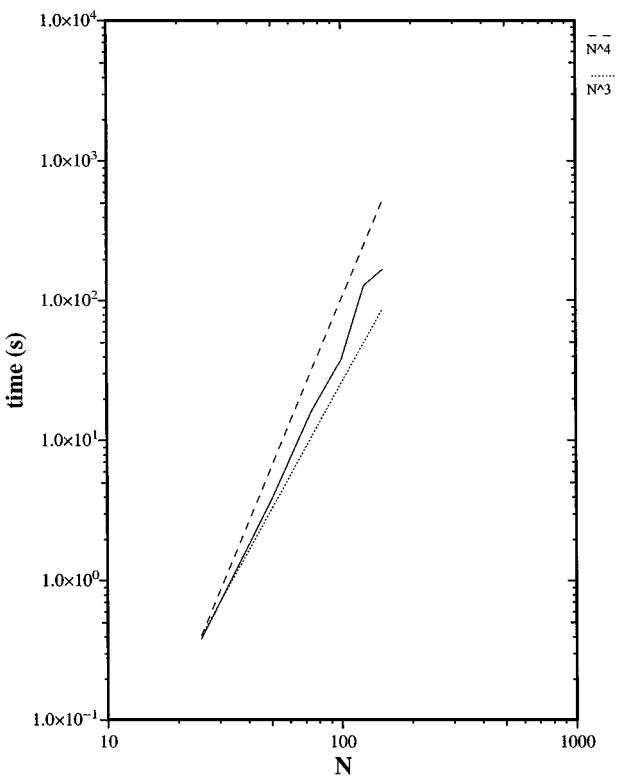

FIG. 4. Execution time vs the number N of unknowns, compared with the slopes N^3 and N^4.

fraction of the total in spite of the complexity of its formulation described in Subsection 3.3. The computational cost is nearly equally divided between the initialization phase (solution of the eigenproblem and evaluation of the basis functions at the Legendre points), the perturbation of the right-hand side, and the solution by means of the triple similarity transformations given in Subsection 3.5. The right-hand side perturbation is always the most expensive part of the solution algorithm but, when the same equation has to be solved for several source functions under identical boundary conditions, this step can be performed once and for all, as well as the other preceding computational steps.

We note that a substantial decrease in the CPU times with respect to the reported figures is achieved by replacing the Fortran 90 MATMUL built-in function by architecture optimized BLAS subroutines. However, a detailed performance comparison of different code implementations of the proposed algorithm, possibly across different platforms, is beyond the scope of the present article.

5. CONCLUSIONS

A new Galerkin–Legendre spectral method for the direct solution of Poisson or Helmholtz equations in three-dimensional rectangular domains under nonhomogeneous Dirichlet condition on the entire boundary has been presented. The method is an extension of Jie Shen's diagonalization algorithm for 2D problems [8] and employs a lifting of the Dirichlet datum to obtain the Legendre coefficients of the trace of the unknown. The lifting is performed in three subsequent steps to account for the values prescribed first at the vertices, then along the edges, and finally on the faces of the rectangular domain, in compliance with the existing compatibility conditions for the Dirichlet data on the six faces of the boundary. The Legendre coefficients associated with the components of the lifting other than the vertex one are determined by the L^2 projection of the boundary values along the edges and on the faces through Gauss–Legendre numerical integration. The solution algorithm fully exploits the direct product nature of the spectral approximation and reduces the solution of the 3D elliptic problem to a sequence of pentadiagonal symmetric linear problems and eigenproblems for the three 1D mass matrices in the Cartesian directions and of similarity transformations. The performed numerical tests illustrate the spectral accuracy of the method and demonstrate the possibility of solving 3D elliptic equations with up $\mathcal{O}(10^7)$ spectral unknowns very efficiently. It must be emphasized that all the algorithmic components of the proposed method are intrinsically vectorial; moreover, owing to the complete independence of the matrix $\times$ array multiplications involved in the triple similarity transformations, a high degree of parallelization of the algorithm is possible, in compliance with its direct product nature.

The present method can be extended to elliptic equations supplemented by the Neumann condition by introducing a different basis which allows us to enforce the derivative boundary condition in an essential way, as suggested by Jie Shen [8]. In this way, the diagonal and pentadiagonal patterns of the 1D stiffness and mass matrices are preserved and a lifting of the Neumann boundary datum is performed, leading to an algorithm with a structure surprisingly similar to that for the solution of the Dirichlet problem, as will be shown in a forthcoming work.

A. APPENDIX

This appendix contains the explicit derivation of the expressions for performing the lifting of the Dirichlet data on the boundary of the 3D rectangular domain. Subsection A.1 recalls

the complete set of discrete boundary values used by the proposed direct solver. These values are required by our algorithm to compute the Legendre coefficients associated with the trace of the unknown by means of L^2 projection through Gauss–Legendre numerical quadrature. Then, Subsections A.2 and A.3 deal with the derivation of the expressions for the components of the lifting associated with the edges and the faces, respectively.

A.1. *The Set of Discrete Dirichlet Data*

Let us first summarize the set of boundary values needed by our spectral solution algorithm for the Dirichlet problem in three dimensions. This set comprises three groups of data. First, there are the values at the eight corners of the cube,

$$\begin{pmatrix} a^{\mathrm{lbn}} & a^{\mathrm{ltn}} & a^{\mathrm{lbf}} & a^{\mathrm{ltf}} \\ a^{\mathrm{rbn}} & a^{\mathrm{rtn}} & a^{\mathrm{rbf}} & a^{\mathrm{rtf}} \end{pmatrix}.$$

Then, there are the values at the (1D) Gauss–Legendre points of the twelve edges of the cube, which we regroup in three sets of four edges parallel to each coordinate axis, namely, for the x axis

$$\begin{cases} \mathcal{A}^{ex_1} = \{a(x_g, -1, -1), 1 \le g \le I+1\} \\ \mathcal{A}^{ex_2} = \{a(x_g, +1, -1), 1 \le g \le I+1\} \\ \mathcal{A}^{ex_3} = \{a(x_g, +1, +1), 1 \le g \le I+1\} \\ \mathcal{A}^{ex_4} = \{a(x_g, -1, +1), 1 \le g \le I+1\} \end{cases}$$

for the y axis

$$\begin{cases} \mathcal{A}^{ey_1} = \{a(-1, y_g, -1), 1 \le g \le J+1\} \\ \mathcal{A}^{ey_2} = \{a(+1, y_g, -1), 1 \le g \le J+1\} \\ \mathcal{A}^{ey_3} = \{a(+1, y_g, +1), 1 \le g \le J+1\} \\ \mathcal{A}^{ey_4} = \{a(-1, y_g, +1), 1 \le g \le J+1\}, \end{cases}$$

and for the z axis

$$\begin{cases} \mathcal{A}^{ez_1} = \{a(-1, -1, z_g), 1 \le g \le K+1\} \\ \mathcal{A}^{ez_2} = \{a(+1, -1, z_g), 1 \le g \le K+1\} \\ \mathcal{A}^{ez_3} = \{a(+1, +1, z_g), 1 \le g \le K+1\} \\ \mathcal{A}^{ez_4} = \{a(-1, +1, z_g), 1 \le g \le K+1\}. \end{cases}$$

Finally, there are the values at the (2D) Gauss–Legendre points of the six faces of the cube, namely

$$\begin{cases} \mathcal{A}^{FX_1} = \{a(-1, y_g, z_h), 1 \le g \le J+1, 1 \le h \le K+1\} \\ \mathcal{A}^{FX_2} = \{a(+1, y_g, z_h), 1 \le g \le J+1, 1 \le h \le K+1\} \\ \mathcal{A}^{FY_1} = \{a(x_g, -1, z_h), 1 \le g \le I+1, 1 \le h \le K+1\} \\ \mathcal{A}^{FY_2} = \{a(x_g, +1, z_h), 1 \le g \le I+1, 1 \le h \le K+1\} \\ \mathcal{A}^{FZ_1} = \{a(x_g, y_h, -1), 1 \le g \le I+1, 1 \le h \le J+1\} \\ \mathcal{A}^{FZ_2} = \{a(x_g, y_h, +1), 1 \le g \le I+1, 1 \le h \le J+1\}. \end{cases}$$

The total number of distinct Dirichlet values is therefore $8+4(I+J+K+3)+2(I+1)(J+1)+2(I+1)(K+1)+2(J+1)(K+1)=2(IJ+IK+JK+4I+4J+4K+13)$. This value can be compared with the number of discrete Dirichlet values which are used instead in a collocation approach based on $(I+1)(J+1)(K+1)$ Gauss–Lobatto points. In this case the number of collocation points on the boundary is $2(IJ+IK+JK+1)$. As a consequence, the proposed Galerkin–Legendre method samples the datum $a(\boldsymbol{r}_{\partial\Omega})$ of the Dirichlet boundary condition at $8(I+J+K+3)$ more points than collocation schemes using the same number of polynomials.

A.2. *Derivation of the Edge Component of the Lifting*

Let us consider the problem associated with the subcomponent of the lifting to account for the Dirichlet data prescribed along the four horizontal edges, once the possibly non-homogeneous values at the vertices have been already taken into account by the corner component of the lifting $\boldsymbol{U}_a^{(\mathrm{c})}$. We introduce the test functions

$$L_i^*(x)L_j^*(y)L_k^*(z), \qquad \text{for } 2\le i\le I,\ j=0,1, \text{ and } k=0,1,$$

and the expansion

$$\begin{aligned} u_{a,N}^{\mathrm{edges}}(x,y,z) = {} & \sum_{i=2}^{I} L_i^*(x)\, U_a^{(\mathrm{h})}(i,j,k)\, L_j^*(y) \sum_{j=0,1} L_k^*(z) \sum_{k=0,1} \\ & + \sum_{i=0,1} L_i^*(x)\, U_a^{(\mathrm{v})}(i,j,k)\, L_j^*(y) \sum_{j=2}^{J} L_k^*(z) \sum_{k=0,1} \\ & + \sum_{i=0,1} L_i^*(x)\, U_a^{(\mathrm{d})}(i,j,k)\, L_j^*(y) \sum_{j=0,1} L_k^*(z) \sum_{k=2}^{K} . \end{aligned}$$

Here the symbol $\sum$ is used for indicating summation in the third dimension z, similarly to the one adopted for the second dimension y, but placed on the top of the summed elements of the three-dimensional matrix. Consider now the uncoupled problem stated in Subsection 3.3.2 for the four horizontal edges,

$$\sum_{\ell=1}^{4} \int_{ex_\ell} v u_{a,N}^{\mathrm{edges}} = \sum_{\ell=1}^{4} \int_{ex_\ell} v\left(a^{ex_\ell} - u_{a,N}^{\mathrm{corners}}\right),$$

and express it in a fully discrete form by taking $v(x,y,z)=L_{i'}^*(x)L_{j'}^*(y)L_{k'}^*(z)$ with $2\le i'\le I$, $j'=0,1$, and $k'=0,1$. By introducing the 2×2 matrix H with elements

$$H_{i,j} = L_i^*(-1)L_j^*(-1) + L_i^*(1)L_j^*(1), \qquad \text{for } i=0,1 \text{ and } j=0,1,$$

and using the elements of the one-dimensional mass matrix, $m_{i',i} = \int_{-1}^{1} L_{i'}^*(x) L_i^*(x)\, dx$, the weak equations become, for every $2 \le i' \le I$, $j' = 0, 1$ and $k' = 0, 1$,

$$\begin{aligned}
&\sum_{i=2}^{I} m_{i',i}\, U_a^{(\mathrm{h})}(i, j, k)\, H_{j,j'} \sum_{j=0,1} H_{k,k'} \sum_{k=0,1} \\
&\quad = \int_{-1}^{1} L_{i'}^*(x)\; a^{ex_1}(x)\; dx\; L_{j'}^*(-1) + \int_{-1}^{1} L_{i'}^*(x)\; a^{ex_2}(x)\; dx\; L_{j'}^*(-1) \\
&\qquad + \int_{-1}^{1} L_{i'}^*(x)\; a^{ex_3}(x)\; dx\; L_{j'}^*(1) + \int_{-1}^{1} L_{i'}^*(x)\; a^{ex_4}(x)\; dx\; L_{j'}^*(1) \\
&\qquad - \sum_{i=0,1} m_{i',i}\, U_a^{(\mathrm{c})}(i, j, k)\, H_{j,j'} \sum_{j=0,1} H_{k,k'} \sum_{k=0,1} .
\end{aligned}$$

In the actual algorithm, the integrals on the right-hand side are evaluated approximately by means of Gauss–Legendre quadrature formula to give, for instance,

$$\int_{-1}^{1} L_{i'}^*(x) a^{ex_\ell}(x)\, dx = \sum_{g=1}^{I+1} L_{i'}^*(x_g)\, w_g\, a^{ex_\ell}(x_g),$$

where x_g and w_g, $1 \le g \le I+1$, are the quadrature nodes and their respective weights. Accordingly, the previous weak equations assume the form

$$\begin{aligned}
&\sum_{i=2}^{I} m_{i',i}\, U_a^{(\mathrm{h})}(i, j, k)\, H_{j,j'} \sum_{j=0,1} H_{k,k'} \sum_{k=0,1} \\
&\quad = \sum_{g=1}^{I+1} L_{i'}^*(x_g) w_g \Big[a^{ex_1}(x_g)\; L_{k'}^*(-1)\; L_{j'}^*(-1) + a^{ex_2}(x_g)\; L_{k'}^*(-1)\; L_{j'}^*(1) + a^{ex_3}(x_g)\; L_{k'}^*(1)\; L_{j'}^*(1) \\
&\qquad + a^{ex_4}(x_g)\; L_{k'}^*(1)\; L_{j'}^*(-1) \Big] - \sum_{i=0,1} m_{i',i}\, U_a^{(\mathrm{c})}(i, j, k)\, H_{j,j'} \sum_{j=0,1} H_{k,k'} \sum_{k=0,1} .
\end{aligned}$$

The whole system can be recast in matrix form by introducing the vector of the Gauss–Legendre weights

$$\mathcal{W} \equiv \{w_g, 1 \le g \le I+1\},$$

the array $\mathcal{L}$ of values of the Legendre functions computed at the Gauss–Legendre nodes, indicated by script symbols, namely,

$$\mathcal{L} \equiv \{\mathcal{L}(g, i) = L_i^*(x_g), 1 \le g \le I+1, 0 \le i \le I\},$$

and using the four vectors $\mathcal{A}^{ex_1}$, $\mathcal{A}^{ex_2}$, $\mathcal{A}^{ex_3}$, and $\mathcal{A}^{ex_4}$, defined in Appendix A.1. The full system in matrix form reads as

$$\begin{aligned}\overset{H}{\boldsymbol{M}}\,\overset{H}{\boldsymbol{U}}{}_a^{(\mathrm{h})} = \mathcal{L}^T \Bigg\{ \mathcal{W} \star \Bigg[& \begin{pmatrix} L_0^*(-1) & L_1^*(-1) \\ & \mathcal{A}^{ex_1} \end{pmatrix} \begin{pmatrix} L_0^*(-1) & L_1^*(-1) \end{pmatrix} \\ & + \begin{pmatrix} L_0^*(-1) & L_1^*(-1) \\ & \mathcal{A}^{ex_2} \end{pmatrix} \begin{pmatrix} L_0^*(1) & L_1^*(1) \end{pmatrix} + \begin{pmatrix} L_0^*(1) & L_1^*(1) \\ & \mathcal{A}^{ex_3} \end{pmatrix} \begin{pmatrix} (L_0^*(1) & L_1^*(1) \end{pmatrix} \\ & + \begin{pmatrix} L_0^*(1) & L_1^*(1) \\ & \mathcal{A}^{ex_4} \end{pmatrix} \begin{pmatrix} L_0^*(-1) & L_1^*(-1) \end{pmatrix} \Bigg] \Bigg\} - M^{(\mathrm{h})}\,\overset{H}{\boldsymbol{U}}{}_a^{(\mathrm{c})} H,\end{aligned}$$

where $\star$ denotes the element-by-element multiplication of vectors and where we introduced the following partitioning of the mass matrix,

$$M = \begin{pmatrix} M^{(\mathrm{c})} & M^{(\mathrm{h})T} \\ M^{(\mathrm{h})} & \boldsymbol{M} \end{pmatrix},$$

using sans serif letters to denote vectors and matrices which pertain only to internal modes, that is, to basis functions vanishing at the extremes of the interval.

In particular, for our basis, the matrix H is diagonal and therefore the system of equations can be written as four fully decoupled systems each of $(I+1)$ unknowns. In fact, for the Legendre basis $L_i^*(x)$ one has

$$H = \begin{pmatrix} 2 & 0 \\ 0 & 1 \end{pmatrix},$$

and the four uncoupled systems to perform the component of the lifting associated with the horizontal edges are

$$\begin{aligned}
\boldsymbol{M}\boldsymbol{U}_a^{(\mathrm{h})}(\cdot,0,0) &= \frac{1}{4}\mathcal{L}^T[\mathcal{W}\star(\mathcal{A}^{ex_1}+\mathcal{A}^{ex_2}+\mathcal{A}^{ex_3}+\mathcal{A}^{ex_4})] - M^{(\mathrm{h})}U_a^{(\mathrm{c})}(\cdot,0,0),\\
\boldsymbol{M}\boldsymbol{U}_a^{(\mathrm{h})}(\cdot,1,0) &= \frac{1}{2\sqrt{2}}\mathcal{L}^T[\mathcal{W}\star(-\mathcal{A}^{ex_1}+\mathcal{A}^{ex_2}+\mathcal{A}^{ex_3}-\mathcal{A}^{ex_4})] - M^{(\mathrm{h})}U_a^{(\mathrm{c})}(\cdot,1,0),\\
\boldsymbol{M}\boldsymbol{U}_a^{(\mathrm{h})}(\cdot,0,1) &= \frac{1}{2\sqrt{2}}\mathcal{L}^T[\mathcal{W}\star(-\mathcal{A}^{ex_1}-\mathcal{A}^{ex_2}+\mathcal{A}^{ex_3}+\mathcal{A}^{ex_4})] - M^{(\mathrm{h})}U_a^{(\mathrm{c})}(\cdot,0,1),\\
\boldsymbol{M}\boldsymbol{U}_a^{(\mathrm{h})}(\cdot,1,1) &= \frac{1}{2}\mathcal{L}^T[\mathcal{W}\star(\mathcal{A}^{ex_1}-\mathcal{A}^{ex_2}+\mathcal{A}^{ex_3}-\mathcal{A}^{ex_4})] - M^{(\mathrm{h})}U_a^{(\mathrm{c})}(\cdot,1,1).
\end{aligned}$$

Notice that, irrespective of such a decoupling, the edge component of the lifting cannot be evaluated on a edge-by-edge base.

A.3. *Derivation of the Face Component of the Lifting*

We consider the problem associated with the subcomponent of the lifting to account for the Dirichlet values on the faces whose normal is oriented as the z-axis, once their edges have been already homogenized by the previous determination of all of the edge components

of the lifting $\boldsymbol{U}_a^{(\mathrm{h})}$, $\boldsymbol{U}_a^{(\mathrm{v})}$, and $\boldsymbol{U}_a^{(\mathrm{d})}$. To express this problem in a discrete form we introduce the test functions

$$L_i^*(x)L_j^*(y)L_k^*(z), \qquad \text{for } 2 \le i \le I,\ 2 \le j \le J, \text{ and } k = 0, 1,$$

and the expansion

$$\begin{aligned} u_{a,N}^{\mathrm{faces}}(x,y,z) = {} & \sum_{i=2}^{I} L_i^*(x)\, U_a^{(\mathrm{D})}(i,j,k)\, L_j^*(y) \sum_{j=2}^{J} L_k^*(z) \sum_{k=0,1} \\ & + \sum_{i=0,1} L_i^*(x)\, U_a^{(\mathrm{H})}(i,j,k)\, L_j^*(y) \sum_{j=2}^{J} L_k^*(z) \sum_{k=2}^{K} \\ & + \sum_{i=2}^{I} L_i^*(x)\, U_a^{(\mathrm{V})}(i,j,k)\, L_j^*(y) \sum_{j=0,1} L_k^*(z) \sum_{k=2}^{K} . \end{aligned}$$

Consider now the uncoupled problem stated in Subsection 3.3.3 for the two faces normal to the z axis,

$$\sum_{\ell=1}^{2} \int_{FZ_\ell} v\, u_{a,N}^{\mathrm{faces}} = \sum_{\ell=1}^{2} \int_{FZ_\ell} v \big(a^{FZ_\ell} - u_{a,N}^{\mathrm{edges}} - u_{a,N}^{\mathrm{corners}} \big),$$

and express it in a fully discrete form by taking $v(x,y,z) = L_{i'}^*(x)L_{j'}^*(y)L_{k'}^*(z)$ with $2 \le i' \le I$, $2 \le j' \le J$ and $k' = 0, 1$. Recalling the 2×2 matrix H introduced previously, using the one-dimensional mass matrix elements $m_{i',i} = \int_{-1}^{1} L_{i'}^*(x) L_i^*(x)\, dx$ and $n_{j',j} = \int_{-1}^{1} L_{j'}^*(y) L_j^*(y)\, dy$, and exploiting the fact that the term pertaining to the d-edges vanishes since $L_k^*(\pm 1) = 0$, $k \ge 2$, the weak equations become, for every $2 \le i' \le I$, $2 \le j' \le J$, and $k' = 0, 1$,

$$\begin{aligned} & \sum_{i=2}^{I} m_{i',i}\, U_a^{(\mathrm{D})}(i,j,k)\, n_{j,j'} \sum_{j=2}^{J} H_{k,k'} \sum_{k=0,1} \\ & \quad = \int_{FZ_1} L_{i'}^*(x)\, a^{FZ_1}(x,y)\, L_{j'}^*(y)\, dx\, dy\, L_{k'}^*(-1) + \int_{FZ_2} L_{i'}^*(x)\, a^{FZ_2}(x,y)\, L_{j'}^*(y)\, dx\, dy\, L_{k'}^*(1) \\ & \qquad - \sum_{i=2}^{I} m_{i',i}\, U_a^{(\mathrm{h})}(i,j,k)\, n_{j,j'} \sum_{j=0,1} H_{k,k'} \sum_{k=0,1} - \sum_{i=0,1} m_{i',i}\, U_a^{(\mathrm{v})}(i,j,k)\, n_{j,j'} \sum_{j=2}^{J} H_{k,k'} \sum_{k=0,1} \\ & \qquad \sum_{i=0,1} m_{i',i}\, U_a^{(\mathrm{c})}(i,j,k)\, n_{j,j'} \sum_{j=0,1} . \end{aligned}$$

In the actual algorithm, the double integrals on the right-hand side are evaluated approximately by means of Gauss–Legendre quadrature formula to give, for instance,

$$\int_{-1}^{1}\int_{-1}^{1} L_{i'}^{*}(x)\, a^{FX_\ell}(x)\, L_{j'}^{*}(y)\, dx\, dy = \sum_{g=1}^{I+1} L_{i'}^{*}(x_g)\, w_g\, a^{FX_\ell}(x_g, y_h) v_h\, L_{j'}^{*}(y_h) \sum_{h=1}^{J+1},$$

where, for $1 \le g \le I+1$ and $1 \le h \le J+1$, x_g and y_h are the quadrature nodes and w_g and v_h and their respective weights. Accordingly, the previous weak equations assume the form

$$\begin{aligned}
&\sum_{i=2}^{I} m_{i',i}\, U_a^{(\mathrm{D})}(i,j,k)\, n_{j,j'} \sum_{k=0,1}^{H_{k,k'}} \sum_{j=2}^{J} \\
&\quad = \sum_{g=1}^{I+1} L_{i'}^{*}(x_g) w_g \left\{ \begin{matrix} L_{k'}^{*}(-1) \\ a^{FZ_1}(x_g, y_h) \end{matrix} + \begin{matrix} L_{k'}^{*}(1) \\ a^{FZ_2}(x_g, y_h) \end{matrix} \right\} v_h\, L_{j'}^{*}(y_h) \sum_{h=1}^{J+1} \\
&\qquad - \sum_{i=2}^{I} m_{i',i}\, U_a^{(\mathrm{h})}(i,j,k)\, n_{j,j'} \sum_{k=0,1}^{H_{k,k'}} \sum_{j=0,1} - \sum_{i=0,1} m_{i',i}\, U_a^{(\mathrm{v})}(i,j,k)\, n_{j,j'} \sum_{k=0,1}^{H_{k,k'}} \sum_{j=2}^{J} \\
&\qquad - \sum_{i=0,1} m_{i',i}\; U_a^{(\mathrm{c})}(i,j,k)\; n_{j,j'} \sum_{k=0,1}^{H_{k,k'}} \sum_{j=0,1} .
\end{aligned}$$

The whole system can be recast in matrix form using the two matrices $\mathcal{A}^{FZ_1}$ and $\mathcal{A}^{FZ_2}$ of the values of the Dirichlet conditions at the Gauss–Legendre quadrature points belonging to the two considered faces, defined in Appendix A.1. The full system in matrix form reads

$$\begin{aligned}
\overset{H}{\boldsymbol{M}}\, \boldsymbol{U}_a^{(\mathrm{D})} \boldsymbol{N} &= \mathcal{L}^T \mathcal{W} \begin{bmatrix} (L_0^*(-1) \quad L_1^*(-1)) & & (L_0^*(1) \quad L_1^*(1)) \\ \mathcal{A}^{FZ_1} & + & \mathcal{A}^{FZ_2} \end{bmatrix} \mathcal{V}\mathcal{J} \\
&\quad - \overset{H}{\boldsymbol{M}}\, \boldsymbol{U}_a^{(\mathrm{h})} N^{(\mathrm{v})} - M^{(\mathrm{h})}\, \overset{H}{\boldsymbol{U}_a^{(\mathrm{v})}}\, \boldsymbol{N} - M^{(\mathrm{h})}\, \overset{H}{\boldsymbol{U}_a^{(\mathrm{c})}}\, N^{(\mathrm{v})},
\end{aligned}$$

with usual meaning for symbols and for matrix partitionings and where we have introduced the two diagonal matrices of the Gauss–Legendre weights,

$$\mathcal{W} = \begin{pmatrix} w_1 & & & \\ & w_2 & & \\ & & \ddots & \\ & & & w_{I+1} \end{pmatrix} \quad \text{and} \quad \mathcal{V} = \begin{pmatrix} v_1 & & & \\ & v_2 & & \\ & & \ddots & \\ & & & v_{J+1} \end{pmatrix}.$$

Since the matrix H is diagonal the system of equations can be written as two fully decoupled two-dimensional consistent matrix problems each of $(I-1) \times (J-1)$ unknowns. Using

the elements of H and rearranging, one obtains two uncoupled systems to perform the component of the lifting associated with two faces orthogonal to the z direction,

$$\begin{aligned}
\mathbf{M}U_a^{(\mathrm{D})}(\cdot,\cdot,0)\mathbf{N} &= \frac{1}{2}\mathcal{L}^T\mathcal{W}(\mathcal{A}^{FZ_1}+\mathcal{A}^{FZ_2})\mathcal{V}\mathcal{J} - \mathbf{M}U_a^{(\mathrm{h})}(\cdot,\cdot,0)N^{(\mathrm{v})} \\
&\quad - M^{(\mathrm{h})}U_a^{(\mathrm{v})}(\cdot,\cdot,0)\mathbf{N} - M^{(\mathrm{h})}U_a^{(\mathrm{c})}(\cdot,\cdot,0)N^{(\mathrm{v})}, \\
\mathbf{M}U_a^{(\mathrm{D})}(\cdot,\cdot,1)\mathbf{N} &= \frac{1}{\sqrt{2}}\mathcal{L}^T\mathcal{W}(-\mathcal{A}^{FZ_1}+\mathcal{A}^{FZ_2})\mathcal{V}\mathcal{J} - \mathbf{M}U_a^{(\mathrm{h})}(\cdot,\cdot,1)N^{(\mathrm{v})} \\
&\quad - M^{(\mathrm{h})}U_a^{(\mathrm{v})}(\cdot,\cdot,1)\mathbf{N} - M^{(\mathrm{h})}U_a^{(\mathrm{c})}(\cdot,\cdot,1)N^{(\mathrm{v})}.
\end{aligned}$$

It is important to remark that, again, irrespective of such a decoupling, the face component of the lifting cannot be evaluated on a face-by-face base.

REFERENCES

1. D. Gottlieb and S. O. Orszag, *Numerical Analysis of Spectral Methods: Theory and Applications* (SIAM, Philadelphia, 1977).
2. C. Canuto, M. Y. Hussaini, A. Quarteroni, and T. A. Zang, *Spectral Methods in Fluid Mechanics* (Springer-Verlag, New York, 1988).
3. J. P. Boyd, *Chebyshev & Fourier Spectral Methods*, Lecture Notes in Engineering (Springer-Verlag, New York, 1989).
4. D. B. Haidvogel and T. A. Zang, The accurate solution of Poisson's equation by expansion in Chebyshev polynomials, *J. Comput. Phys.* **30**, 167 (1979).
5. P. Haldenwang, G. Labrosse, S. Abboudi, and M. O. Deville, Chebyshev 3D spectral and 2D pseudospectral solvers for the Helmholtz equation, *J. Comput. Phys.* **55**, 115 (1984).
6. C. Bernardi and Y. Maday, *Approximations spectrales des problèmes aux limites elliptiques* (Springer-Verlag, Paris, 1992).
7. A. Quarteroni and A. Valli, *Numerical Approximation of Partial Differential Equations* (Springer-Verlag, Berlin, 1997), 2nd ed.
8. Jie Shen, Efficient spectral-Galerkin method. I. Direct solvers of second- and fourth-order equations using Legendre polynomials, *SIAM J. Sci. Comput.* **15**, 1489 (1994).
9. Jie Shen, Efficient spectral-Galerkin method. II. Direct solvers of second- and fourth-order equations using Chebyshev polynomials, *SIAM J. Sci. Comput.* **16**, 74 (1995).
10. F. Auteri and L. Quartapelle, Galerkin spectral method for the vorticity and stream function equations, *J. Comput. Phys.* **149**, 306 (1999).
11. G. Strang and G. J. Fix, *An Introduction to Finite Element Method* (Prentice Hall, Englewood Cliffs, NJ, 1973).
12. R. E. Lynch, J. R. Rice, and D. H. Thomas, Direct solution of partial difference equations by tensor product methods, *Numer. Math.* **6**, 185 (1964).
13. P. Grisvard, *Elliptic Problems in Nonsmooth Domains* (Pitman, London, 1985).
14. E. Anderson *et al.*, *LAPACK* (SIAM, Philadelphia, 1995), 2nd ed.